A STUDY OF CURRENT VOLTAGE CHARACTERISTICS OF OPEN BASE TRANSISTORS IN CURRENT MODE SECOND BREAKDOWN

623.815
1990
SOH

BY

S. M. SOHEL IMTIAZ

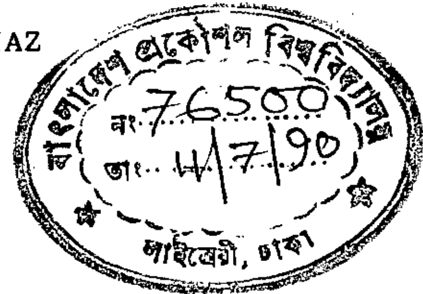

A THESIS

SUBMITTED TO THE DEPARTMENT OF ELECTRICAL AND ELECTRONIC ENGINEERING IN PARTIAL FULFILMENT OF THE REQUIREMENTS FOR THE DEGREE OF

MASTER OF SCIENCE IN ENGINEERING

DEPARTMENT OF ELECTRICAL AND ELECTRONIC ENGINEERING

BANGLADESH UNIVERSITY OF ENGINEERING AND TECHNOLOGY, DHAKA

APRIL, 1990

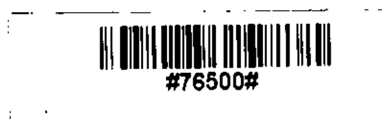

Accepted as satisfactory in partial fulfilment of the requirement for the degree of Master of Science in Engineering (Electrical and Electronic).

BOARD OF EXAMINERS

1.	(Dr. M. M. Shahidul Hassan) Associate Professor Department of Electrical and Electronic Engineering, BUET, Dhaka.	Chairman (Supervisor)
2.	18.4.1990 (Dr. Md. Abdul Matin) Professor and Head Department of Electrical and Electronic Engineering, BUET, Dhaka.	Member (Ex-Officio)
3.	(Dr. A. B. M. Siddique Hossain) Professor Department of Electrical and Electronic Engineering, BUET, Dhaka.	Member
4.	(Dr. Mohammed Ali Choudhury) Assistant Professor Department of Electrical and Electronic Engineering, BUET, Dhaka.	Member
5.	(Dr. Md. Giasuddin Ahmad) Professor Department of Physics, BUET, Dhaka.	Member (external)

CERTIFICATE

This is to certify that this work has been done by me and it has not been submitted elsewhere for the award of any degree or diploma.

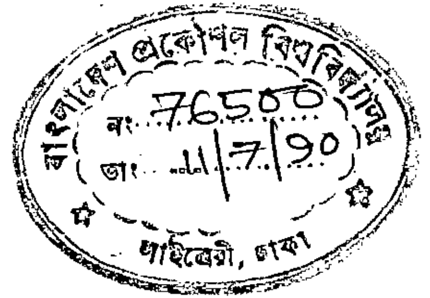

Countersigned

(Dr. M. M. Shahidul Hassan)

Supervisor

Signature of the student

(S. M. Sohel Imtiaz)

ACKNOWLEDGEMENT

The author wishes to express his heartiest gratitude and profound indebtedness to his supervisor Dr. M. M. Shahidul Hassan, Associate Professor of the department of Electrical and Electronic Engineering, Bangladesh University of Engineering and Technology, Dhaka for his supervision, interest, contribution to new ideas and constant guidance throughout the course of this work. Without his whole hearted supervision, this work would not have been done.

The author also wishes to express his thanks and gratitude to Dr. Md. Abdul Matin, Professor and Head of the department of Electrical and Electronic Engineering, BUET for allowing the author to work with the departmental facilities and providing him every help and co-operation at every stage.

The author acknowledges the help and suggestions offered to him by his colleagues of the faculty. In particular, the names of Mr. A. H. M. Zahirul Alam and Mr. Monjurul Haque are to be mentioned and he is indebted to them for their timely help and valuable suggestions.

Acknowledgement is also due for the staffs of the faculty of Electrical and Electronic Engineering who took the trouble of helping the author in preparing the manuscript of the work.

ABSTRACT

Bipolar transistors are prone to failure due to the occurrence of second breakdown. Therefore, studies of second breakdown are very important. This study has examined the mechanism of current mode second breakdown in bipolar junction transistors under open base condition. The field distortion within the collector arising from mobile space charge causes collapse of terminal voltage. The role of the electric field in different regions of the collector on lowering the terminal voltage has been investigated in open-base transistors. Analytical expressions for voltages in different regions within the collector have clearly revealed that the region where the electrons and holes move with their saturated velocities and where the carrier generation is small, is the main contributor to the negative characteristics and is responsible for causing the experimentally observed low holding voltage. It is shown that the holding voltage is a function of collector epitaxial layer thickness. This result verifies the experimental observations that the holding voltage increases with the increase of collector epitaxial layer thickness. The analytical results also upholds the experimental observation that the holding voltage is independent of doping density. This phenomenon initiates at a current density J exceeding space charge limited current density J_O. For current density J greater than J_O, the peak electric field shifts from the base collector metallurgical junction to the collector substrate interface. And at large current densities, avalanche starts at the collector substrate interface. By a substantial increase of doping at the collector substrate interface, it may be possible to initiate this mechanism at very large current density J_O and thereby possible to save this device from permanent damage.

CONTENTS

CHAPTER 1 INTRODUCTION

1.1 Second Breakdown 1

1.2 Thermal Mode Second Breakdown (TSB) 3

1.3 Current Mode Second Breakdown (CSB) 7

1.3.1 Background 7

1.3.2 Development of the Theory of CSB 10

1.4 Summary of the Dissertation 13

CHAPTER 2 CURRENT VOLTAGE CHARACTERISTICS OF EPITAXIAL BIPOLAR TRANSISTOR OPERATING IN CSB UNDER OPEN BASE CONDITION

2.1 Introduction 17

2.2 Theory of Current Mode Second Breakdown 19

2.3 Analytical Expression for Multiplication Factor of Transistor Driven in CSB 30

2.4 Numerical Solution 31

2.4.1 Boundary Values of Electric Field 33

2.4.2 Numerical Techniques Used in Computation of Electric Field and Current Density 34

2.4.3 Features of Numerical Results 36

2.5 Conclusions 37

CHAPTER 3 ANALYTICAL SOLUTION

3.1 Introduction 38

3.2 Analysis 38

3.2.1 Region 1 41

3.2.2 Region 2 48

3.2.3 Region 3 51

3.2.4 Region 4 52

3.2.5 Region 5 54

3.2.6 Region 6 59

3.3 Conclusions 61

CHAPTER 4 CONCLUSIONS 65

BIBLIOGRAPHY 67

APPENDIX A Calculation of Electric Field E_2 70

APPENDIX B Calculation of Maximum Electric Field E_m 71

LIST OF FIGURES

1.1. Collector current vs. collector-emitter voltage under second breakdown condition. 2

1.2. Temperature (T) and current density (J) distributions in (a) normal operation and (b) electro-thermal runaway condition. 5

1.3. (a) Transistor test circuit (b) Typical current-voltage curve. 8

1.4. Central injection from returning avalanche current. 12

1.5. I-V characteristics obtained on small area mesa n^+pnn^+ epitaxial transistors pulsed into current mode second breakdown. 12

2.1. Collector current vs. collector emitter voltage under second breakdown condition. 20

2.2. Field profiles within the collector region 23

2.3. (a) Idealized velocity-field characteristics for holes and electrons. 25

(b) If E_a is the field at the base region then any change in E does not change electron or hole densities so the dE/dx remains zero.

(c) If E_b is the field at the base region then any increase in E implies that dE/dx becomes positive - a total contradiction of the requirement that dE/dx is negative.

(d) With E_C at the base, any change in E gives a negative dE/dx and the field grows rapidly to a high value where avalanche injection starts.

2.4. Field profile for CSB with an extended low field region. 27

2.5. Schematic diagram for second breakdown with strong recombination. 29

2.6. Electron and hole current density as a function of distance. 35

2.7. Field distribution for various current densities. 35

3.1. An $n^+pn^-n^+$ structure. 39

3.2. Electric field profile in the collector region. 39

3.3. Comparison of analytically calculated field with numerical results 58

3.4. J-V characteristics for various epitaxial layer thickness. 62

3.5. Holding voltage vs. epitaxial layer thickness curve. 63

LIST OF SYMBOLS

$b = \frac{\mu_p}{\mu_n}$

$D_n(D_p)$ = electron (hole) diffusion co-efficient, cm^2/s

E = Electric field, V/cm.

E_c, E_1, E_1,E_s, E_2, E_m = Electric field at $x=x_1$, x_2,x_3, x_4, x_5, L respectively.

$E_s = E\ (v_n = v_p = v_s)$

g = generation rate density, $cm^{-3}\ s^{-1}$

J = total current density, A/cm^2.

$J_o = q\ V_s\ N_{DC}$.

J_{ni} = electron current density injected into collector from base.

J_{pi} = hole current density injected into base from collector.

$J_{ns}(J_{ps})$ = electron (hole) current density in region 2.

$L_a = \sqrt{\frac{2V_t\mu_p\tau_p}{1+b}}$ = ambipolar diffusion length.

L = Collector epitaxial layer thickness.

M_n = Electron multiplication factor.

N_{DC} = Collector doping concentration, cm^{-3}.

n(P) = electron (hole) free carrier density.

$n_s(p_s)$= Electron (hole) free carrier density in region 3.

q = Elementary charge, coulomb.

$v_n(v_p)$ = Electron (hole) drift velocity, cm/s.

v_s = Electron and hole scattering limited velocity, cm/s.

x_1, x_2, x_3, x_4, x_5 = boundary of the first, second, third, fourth and fifth regions respectively.

CHAPTER 1

INTRODUCTION

1.1. Second Breakdown

The modern era of solid state Electronics was ushered by the invention of bipolar transistor in the late 40's. It has shown an enormous impact on virtually every area of modern life. However, the power handling capabilities of transistors are limited. One of the reasons for this limitation is a phenomenon known as "Second Breakdown". The term "Second Breakdown" is used for any spontaneous and abrupt reduction in collector-emitter voltage as the collector current is increased (Fig.1.1). Its initiation is manifested by abrupt reduction in the device voltage and a simultaneous constriction of the current. The decrease in voltage with the usual attendant increase in current can cause the malfunction of the circuit, while the internal current constriction will cause localized heating which, in turn, can result in device degradation or even destruction of the device.

The Second Breakdown phenomenon in transistors was first observed by Thornton and Simmons [1] in 1958. They described it as a new type of solid state phenomenon which appears as an abrupt transition to a low voltage circuit mode at high current

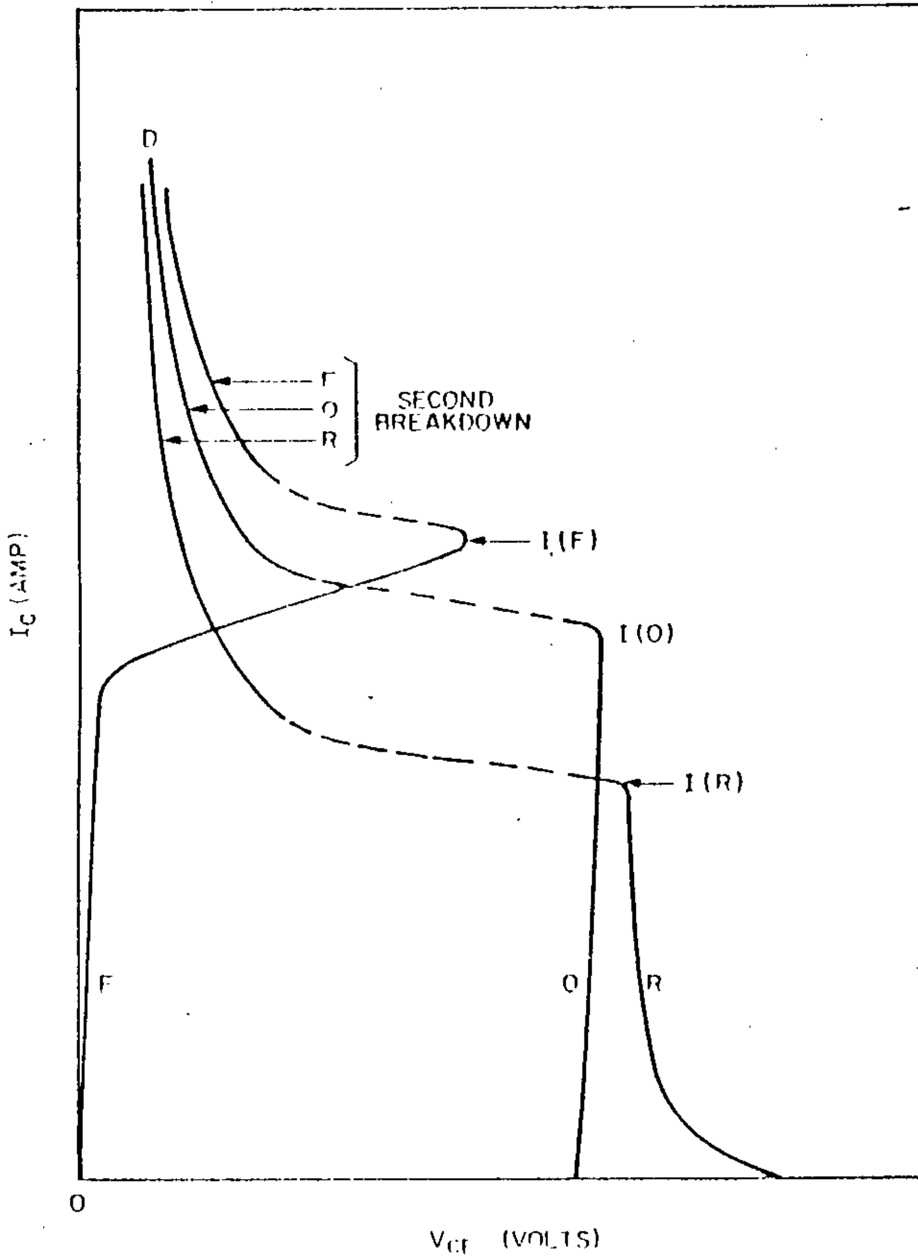

Fig.1.1. Collector current vs. collector-emitter voltage under second breakdown condition. F, O, R, indicates forward-, zero, reverse-base drive, respectively. I and D indicate the initiation of instability and destruction, respectively.

densities under appropriate conditions. They tried to establish it as a bulk, rather than a surface effect. Because of its practical implications, second breakdown has been the subject of extensive study. There are two possible mechanisms to initiate second breakdown: thermal heating and current injection. These two mechanisms will be discussed in the next two sections.

1.2. Thermal mode second breakdown (TSB)

Thermal mode second breakdown has been extensively investigated for a number of years by number of workers. Considerable progress has been made in the area of 'thermal breakdown'. When a certain critical temperature has been reached within the active region of the device, then the thermal mode second breakdown (TSB) is induced by a local regenerative thermal runaway [2]. TSB is initiated by the current filamentation or inhomogeneities in the device structure. It is generally observed when there is avalanche current present although it may occur below the breakdown voltage.

Thermal mode second breakdown can be illustrated as follows. Initially current flows uniformly in the transistor and then a perturbation increases the current at a point. As a consequence the local temperature will increase at that point. The collector

current density will tend to increase according to a positive temperature co-efficient. Consequently collector current density will tend to decrease in the rest of the device. The current will be concentrated in the hottest area if the temperature distribution is heterogeneous. This will lead to further heating of that area. As a result, thermal mode second breakdown will occur due to the development of lateral thermal instability provided the gain of the positive feedback loop in temperature and current density at the hot spot exceed unity. However, the transverse voltage due to the base current flow strongly influence the runaway condition [2]. The role of the base current is schematically illustrated in Fig. 1.2. In normal operation, at a moderate level of power dissipation and temperature within the active area of the device, the current distribution would tend to concentrate towards the centre of the structure due to the spreading of heat flow within the crystal [3]. This is counteracted by the tendency of current to crowd at the emitter periphery by the biasing effect of the centripetal base current flow [Fig. 1.2a]. Distributed base resistance has a stabilizing influence in this case. However, if the local temperature increases for any reason (increase in collector-emitter voltage and consequently in dissipated power, self heating or ambient heating), the thermally generated current flowing through the collector bulk and space charge regions progressively substitutes for the normal current. Moreover, at

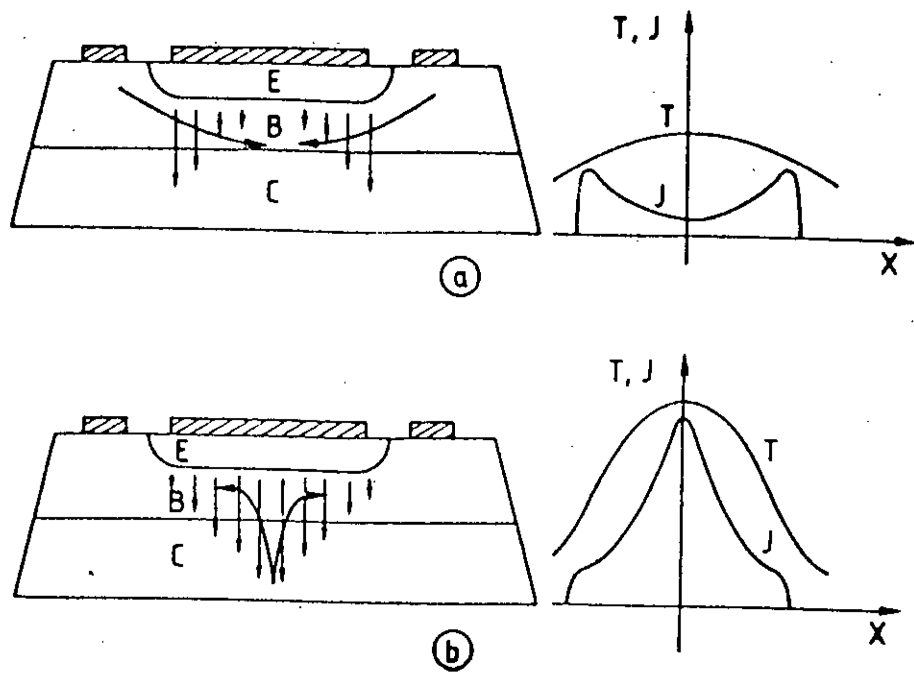

Fig.1.2 Temperature (T) and current density (J) distributions in (a) normal operation and (b) electro-thermal runaway condition.

sufficiently high temperature, the base current will be concentrated in the hottest area, enhancing the trend of the emitter and collector current distributions to concentrate towards the centre of the structure (Fig. 1.2b). As a consequence, instability develops quickly.

The foregoing discussion, which can be transposed to the case of a hot spot in a real structure, suggests that the critical temperature at which an electro-thermal runaway can locally develop is such that the thermally generated (reverse) current flowing from the collector base junction in the hot area may assume the role of the normal base current in this area, supplying the needs of emitter injection and base transport. The critical temperature is thus high and increases as the collector current level increases (upto 400°C in the active region of operation), and all the more the current gain falls at high current densities. In normal operation as the emitter periphery is active, interdigitation favours the temperature homogeneity over the crystal [4] area and one may conclude that the power dissipation capability of the device (or the energy it can absorb under transient conditions) is higher in the high-current low voltage range than in the opposite case.

1.3. Current Mode Second Breakdown (CSB)

1.3.1. Background

It has been mentioned in the previous section that thermal mode second breakdown was thoroughly investigated but less effort has been devoted to current mode second breakdown, particularly for epitaxial bipolar transistor operating under open-base condition. Actually localized thermal effects, which are associated with second breakdown, play a minor role in the initiation of the transition to a low voltage state. The current mode second breakdown phenomenon (CSB) is observed as an abrupt reduction in the voltage drop across the transistor at high current densities under specified conditions. For common emitter PNP transistor, the output characteristics are shown in Fig.1.3. The region between points A and B is predicted from the classical theory of avalanche breakdown. As the current is increased beyond point B, a critical current is reached (point C) where the drop across the transistor suddenly decreases to a low value (point D). As the current is further increased, the voltage drop across the transistor remains low and relatively constant (region D to E). The critical current at which the voltage drop takes place has been designated as I_m. At this current I_m, second breakdown occurs at point D and the current continues to increase but the voltage remains the same.

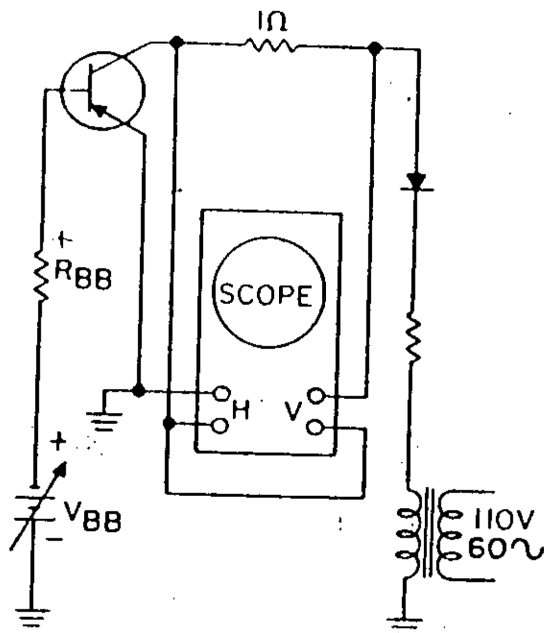

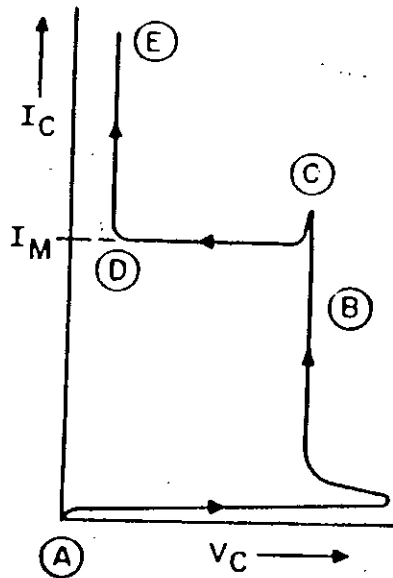

Fig.1.3. (a) Transistor test circuit (b) Typical current-voltage curve.

The increase in the field with a local increase in current can be considered to be the result of very high current densities such that the mobile charge carriers can no longer be considered negligible in the depletion layer. Then conductivity modulation will take place and depletion layer will shrink in width. Since the voltage remains constant, the field must increase. When the local field reaches such a high value that the depletion layer can be sustained no longer and the nature of collector contact is modified grossly, the breakdown occurs at I_m. Because of the localized nature of current carrying path, the carrier density may be extremely high, resulting in a very high local power dissipation and possible localized melting at the semiconductor material.

As a consequence of the high injection efficiency of the emitter electrode, a considerably larger quantity of electron will be injected at the emitter and a much larger quantity of current will flow through the transistor. The significant point is that the part of the base current which flows radially outward under the emitter through the base causes a voltage drop which has the effect of increasing the emitter forward bias toward the center relative to the outer periphery. Thus, the majority carrier current density is concentrated toward the center of the emitter. This effect is termed as " pinch in" effect.

1.3.2. Development of the theory of CSB

An alternative theory for the explanation of second breakdown was proposed by Grutchfield and Moutoux [5] in 1966 and was extended by Hower and Reddi [6] in 1970 by further consideration of the final low voltage state. Epitaxial $n^{+}pn^{-}n^{+}$ bipolar transistors are susceptible to failure from current mode second breakdown (CSB).

CSB is a non-thermal mechanism. It occurs when the collector current density exceeds a certain critical value while the device sustains high voltages. The explanation involves the role of the free carrier space charge in the depletion layer of the collector base junction. At high current densities, this free charge cannot be disregarded in relation to the charged impurities. When the collector current density exceeds the space charge limited current $J_o = qV_s N_{DC}$, where V_s is the saturated carrier velocity, the maximum of the electric field intensity no longer occurs at the metallurgical junction but at the interface between the lightly doped collector region and the highly doped substrate. This maximum electric field increases with the collector current density and may reach values leading to avalanche multiplication. Current crowding occurs at the centre of the emitter in this condition of operation with avalanche

current in the collector. The crowding is caused by higher forward voltage of the base emitter junctions than the edge. Even if the device is initially in a state where there is no external base emitter bias and no emitter injection, with sufficient avalanche current the potential at the centre of the base is high enough to turn the centre of the base emitter junction ON. This condition is shown in [Fig. 1.4]. This injected current, in turn, multiplied in the collector, increasing the base current and reinforcing the central crowding. Hence, by regenerative action, the current increases rapidly and at the same time, is confined to a narrower area. It is believed that regenerative nature of these mechanisms will ultimately allow high current densities to be reached within the centre region causing in a circuit incorporating a collector load resistance, a fall in collector voltage. This condition leads ultimately to the low voltage state associated with current mode second breakdown. The final voltage is below BV_{CEO} (where $M_n=1$). Holes generated by impact ionization near the collector substrate interface not only produce a strong emitter base forward bias voltage but at the same time neutralize the charge of electrons and thereby decrease the electric field in regions outside the avalanche injection zone [6]. As a result the terminal voltage decreases with increase of current density. Fig.1.5 shows the experimentally observed I-V characteristics of three mesa transistor of different sizes (7).

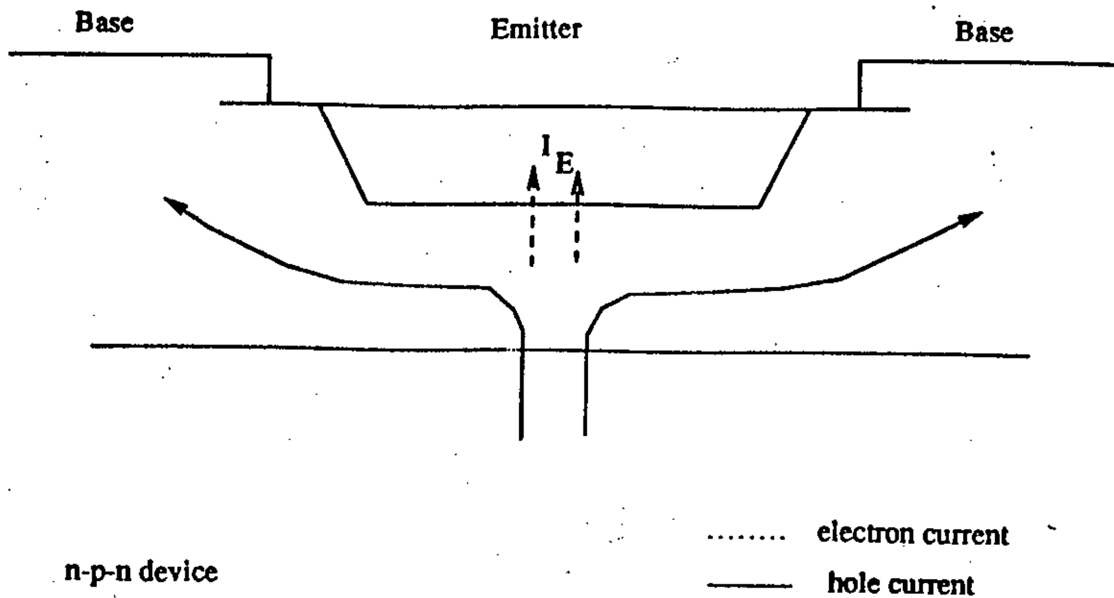

Fig.1.4. Central injection from returning avalanche current.

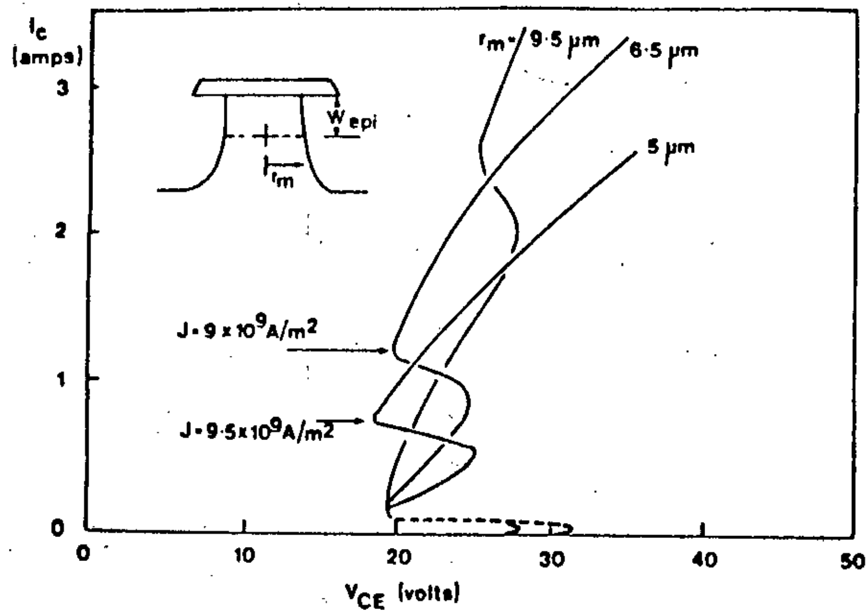

Fig.1.5. I-V characteristics obtained on small area mesa n^+pnn^+ epitaxial transistors pulsed into current mode second breakdown.

The above mentioned two basic mechanisms often interact so that a thermally induced internal current redistribution can produce the conditions required for avalanche injection to occur [8,9]. Once these are established, the electronic mechanism acts very rapidly, since no additional heating is required . Its effect, however , is to accelerate the internal temperature rise and hence the transfer to a thermally activated second breakdown condition.

1.4. Summary of the Dissertation

At the very beginning, bipolar transistors were used for low power rating (<100 W). Now-a-days they have become the competitors of thyristor with a power application of 50-100 KVA by the help of continuous progress in the field of technology, transistor physics and design procedures. In particular, the control of deep diffusions and thick epitaxies with low impurity concentrations has led to great improvements in structure designs. Thus, bipolar transistors have now come of age and are already the preferred devices for a variety of applications, i.e. choppers, inverters, microwave devices, submarine cable transistors, etc. Conversely, second breakdown imposes a limit on the current handling capabilities of bipolar transistors, especially when their voltage blocking capability is high.

Success in solving second breakdown both theoretically and experimentally was achieved partially. Progress has been made in the area of TSB. The identification of localized thermal runaway and the associated theory has led to the design of transistors in which individual emitter resistor limit the formation of regions of high current density over which the device is thermally stable. But so far no success has been achieved in controlling current mode second breakdown. At large collector voltage, transistors are still susceptible to this undesirable phenomenon, whose predominant feature is the transition to a low voltage high current mode occurring at some critical point in the collector characteristics.

So far number of researchers dealt with CSB [5,6,8,9] but the detailed current voltage characteristics are not considered. The main feature of this thesis is to study theoretically these characteristics. An analytical solution has been obtained in the past by taking the following assumptions:

* equal ionization rates for electrons and holes.
* a functional dependence for $\alpha(E)$ that can be readily integrated.
* Constant critical electric field that initiates avalanche ionization.
* The maximum allowed electron multiplication factor on electrostatic grounds which is equal to $M_n = 2$.

* equal mobilities for electrons and holes.

The first one is a poor approximation for silicon. Current voltage characteristics of Si transistors considering different mobilities for electrons and holes were studied by Carroll and Probert [10] but no detailed analysis was given either in the low field region or in the high field region. In the avalanche region near the collector-substrate interface, the field departs from linearity. The point where the field changes its slope can, therefore, be more accurately described by the generation which creates this disturbance on the charge density, rather than the point where the field reaches a critical value.

In chapter 2, electric field, collector length, electron current density and voltage across the high field collector region are computed numerically by Runge -Kutta initial value method. Numerically evaluated field distribution with collector region is compared with the distribution obtained analytically and is found in good agreement with analytically calculated field distribution.

In chapter 3, an analytical model considering different ionization rates, different mobilities of electrons and holes and the effect of generation of carriers on electric field distribution with the avalanche injection region is derived. In

the model, the analytical expressions of voltage for low field region is also obtained under open-base operating condition of $n^+pn^-n^+$ transistor. The results explain the abrupt transitions of the J-V characteristics when the device goes into CSB.

CHAPTER 2

Current Voltage Characteristics of Epitaxial Bipolar Transistor Operating in CSB Under Open Base Condition

2.1. Introduction

In this chapter a study of the distribution of electric field within the collector region of epitaxial bipolar transistor under post avalanche injection conditions is described. The three dimensional nature of the current flow in a transistor presents severe modeling difficulties unless there is recourse to a large scale finite difference scheme. This was avoided because it was felt that such an analysis would be unnecessarily elaborate. Moreover, a one-dimensional analysis was found good enough to be significant to identify the breakdown mechanism that lead to current confinement and explain the abrupt decrease in terminal voltage.

Epitaxial bipolar transistor switches from normal active operational state into a new one characterized by an increase in current and a reduction in voltage having certain critical values of voltage and current [3,5,11,12]. It is widely known as second breakdown and it will destroy the transistor if the high

current is allowed to continue [10]. The sustained low voltage as the current increases abruptly is called the holding voltage. Second breakdown, initiated by pulses of voltage or current is referred to as current mode second breakdown [5,6]. This was necessary to distinguish it from thermal mode second breakdown [13] that is the main topic for example in Schaffts [13] classic review. So it is of absolute necessity to study second breakdown in general and current mode second breakdown in particular. A one dimensional analytical model for current mode second breakdown is developed, using the regional approximation method to evaluate the field in the collector region and the J-V characteristics of the epitaxial bipolar transistor under open base operating conditions. In the collector region , diffusion, recombination and avalanche injection are studied to clarify the physics of the phenomenon. At first the Electric field distribution and J-V characteristics are numerically calculated and then the analytical model with various approximations are developed. The results are in good agreement with numerical values.

Hower and Reddi [6] used an n^+nn^+ diode as a model to understand CSB in transistor. The n^+n contact blocks egress of holes and therefore, behaves differently from a pn^- (base- collector) junction. Dunn and Nuttall [9] have analyzed CSB under open-base condition only for high field region but the role of low field

region was not taken into account. An analytical model is proposed to explain the collapse of the collector-emitter voltage on epitaxial layer parameters. It also shows the existence of current mode negative differential resistance. In this work, a regional approximation method is applied to describe the behavior of the device in the low field region, where avalanche generation of carriers is absent, as well as in the high field region in presence of avalanche multiplication, so that the entire J-V characteristics is obtained.

2.2. Theory of Current Mode Second Breakdown

The use of power transistors and other semiconductor devices is often limited by second breakdown whose initiation is manifested by an abrupt decrease in device voltage with a simultaneous internal constriction of current. For high power transistors it is important to operate the device within a certain safe region so that one can avoid the permanent damage caused by the second breakdown. So it is of utmost importance to study the current-voltage characteristics curve. The general features of the I_C versus V_{CE} characteristics of a transistor under second breakdown conditions are shown in Fig.1.1 [for ready reference, it is reproduced in this chapter (Fig.2.1)]. The symbols F,O,R stand respectively for constant forward-, zero-,

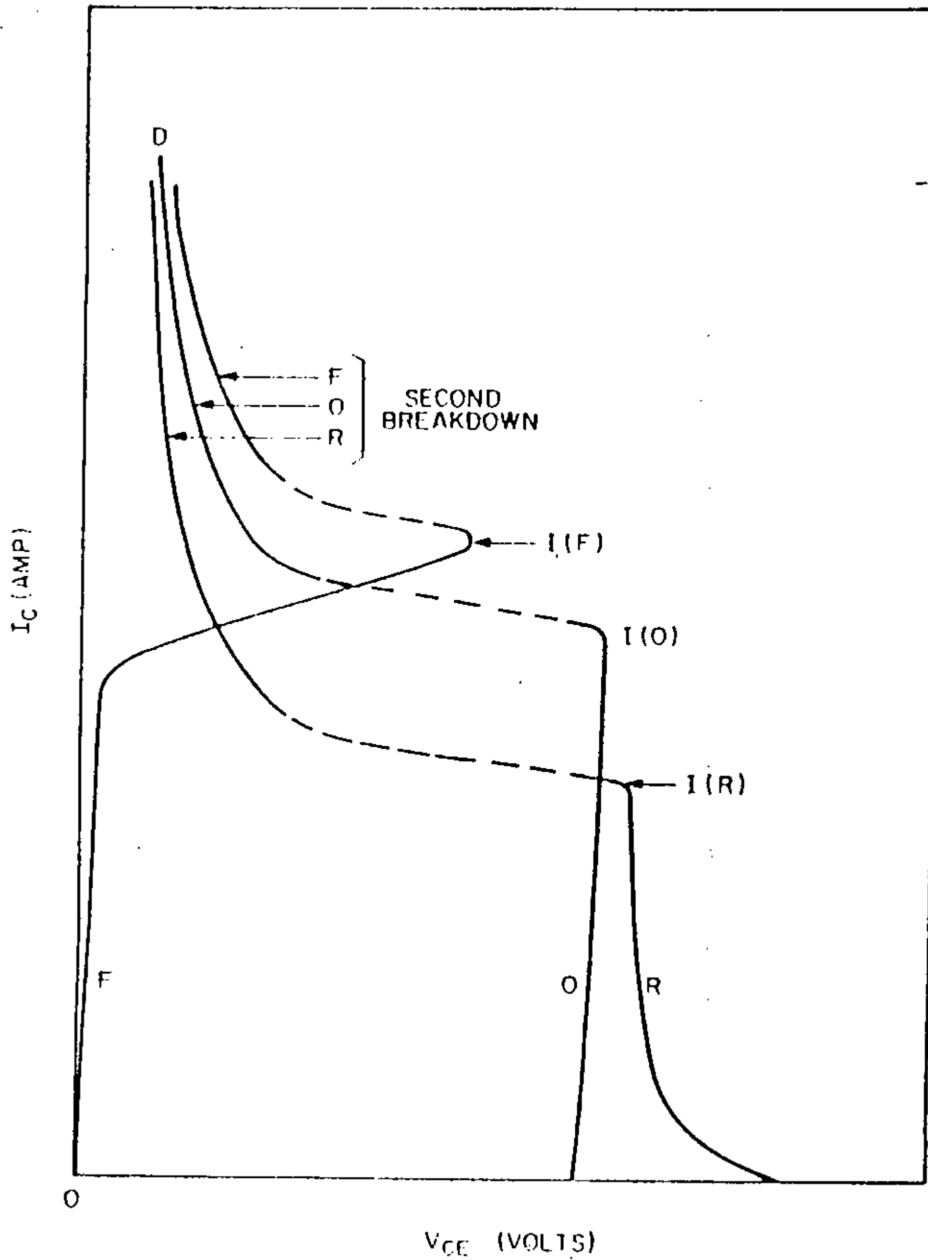

Fig.2.1. Collector current vs. collector emitter voltage under second breakdown condition F, O, R, indicates forward -, zero, reverse-base drive, respectively. I and D indicate the initiation of instability and destruction, respectively.

and reverse-base current drive. For forward-base current, collector current at first increases abruptly and then linearly upto I(F). For zero-base current, I_C increases abruptly at a high collector-emitter voltage V_{CE} upto I(O). The collector current initiates at very high V_{CE} under reverse-base current drive and I_C increases upto I(R) and V_{CE} decreases. The initiation of second breakdown for each of the three base drive conditions is indicated by the abrupt drop in V_{CE} at the instability points I(F), I(O) and I(R). The experimental results can generally be treated as consisting of four stages: the first stage leads to instability, I, at the breakdown or break-over voltage, the second, the switching from the high-voltage to the low-voltage region, the third to the low voltage high current range ; the fourth stage to destruction as marked by D. In this thesis, the reverse-base current drive will be treated first and then the same theory will be extended for the open-base condition.

Now, it will be shown that the peak electric field occurs at base-collector (pn^-) interface at low current density and it shifts to the collector-collector (n^-n^+) interface at high current density. Moreover, there is an extended low field region at the base-collector (pn^-) interface.

For this reason, the boundary conditions and its link with Kirk effect (14) are presented here for discussion with the help of

[Fig.2.2]. In both second breakdown and the Kirk effect it is asserted that the peak electric field is shifted from the base-collector (pn^-) interface to the collector-collector (n^-n^+) interface as the peak current density changes from less than $J_o = qN_{DC}V_s$ to more than J_o [Fig.2.2(a) & (c)]. However, there is an important difference. In the Kirk effect, the injected carrier density is forced to be high by enough current being injected by the emitter. In second breakdown, the peak current density is maintained by impact ionization generating holes which are returned in sufficient numbers, to the base. Actually, under reverse bias operating conditions when $J>J_o$, holes generated by impact ionization near the n^-n^+ contact are returned in sufficient numbers to the base and produce a voltage drop along the base. This has the effect of producing a strong emitter-base forward bias voltage and concentrating the current at the centre of the emitter diffusion. If the holding voltage in the current mode second breakdown is to be as low as experiments indicate [10], then there must be an extended low field region where $\frac{dE}{dx} \approx 0$ and avalanche multiplication is negligible. However, $\frac{d^2E}{dx^2}$ must be positive so that the field can eventually rise to levels at which impact ionization may occur, near the collector contact. If the recombination and diffusion of holes out of the base are neglected, then these requirements fix the values of E that can occur at the boundary of this low field region.

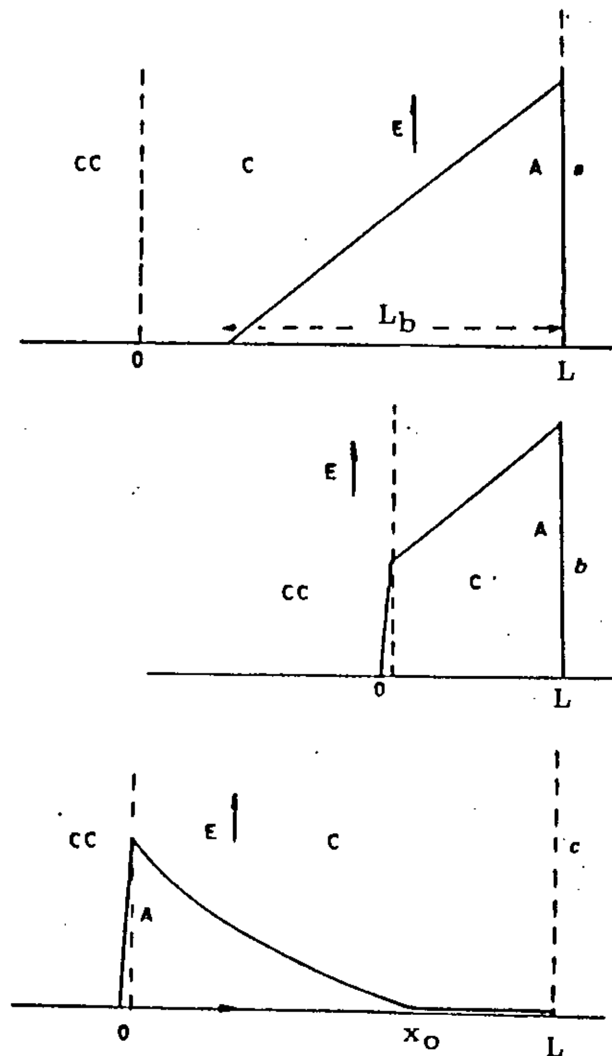

Fig.2.2. Field profiles within the collector region
(a) Field profiles in primary breakdown at low currents, L_b is the depletion distance where L is the thickness of collector layer C. CC is the collector contact and B is base region of transistor.

(b) Here $L = L_b$ so that 'collector reach through' is achieved at breakdown. A marks the avalanche zone.

(c) Secondary breakdown form an extended low-field region from $x = x_o$ to $x = L$

Carroll and Probert have analyzed the range of values of E at the boundary [10]. Idealized velocity-field characteristics for electrons and holes in Si are shown in [Fig.2.3]. If the lowest value of electric field in the extended low-field region was E_a, then both electrons and holes move at their scattering limited velocity V_s [Fig.2.3(b)]. Electrical neutrality would be required for $\frac{dE}{dx}=0$. But any changes in the field would not alter the velocities of the carriers so that the current continuity of each carrier would ensure that the densities remained unaltered for any change in field. This would thus keep $\frac{dE}{dx}$ zero showing that $\frac{d^2E}{d^2x}$ could not be positive. Recombination of the returning holes would only cause the field to fall towards CC rather than rise because the electron density would decrease relative to the hole density as one moved towards CC,controlling the sign of $\frac{dE}{dx}$ through the Gauss equation. Impact ionization would cause the field to rise from a value E_a but this would imply that E_a was already close to the breakdown field strengths rather than well below them.

Again with the requirement of $\frac{dE}{dX}=0$ and neglecting recombination, a low uniform value of E_b is unsatisfactory. Since the electrons have a higher mobility than holes, any increase in the field will reduce the electron density more than it reduces the hole density. From Poission's equation,

$$\epsilon\frac{dE}{dx}=q(p+N_{DC}-n) \tag{2-1}$$

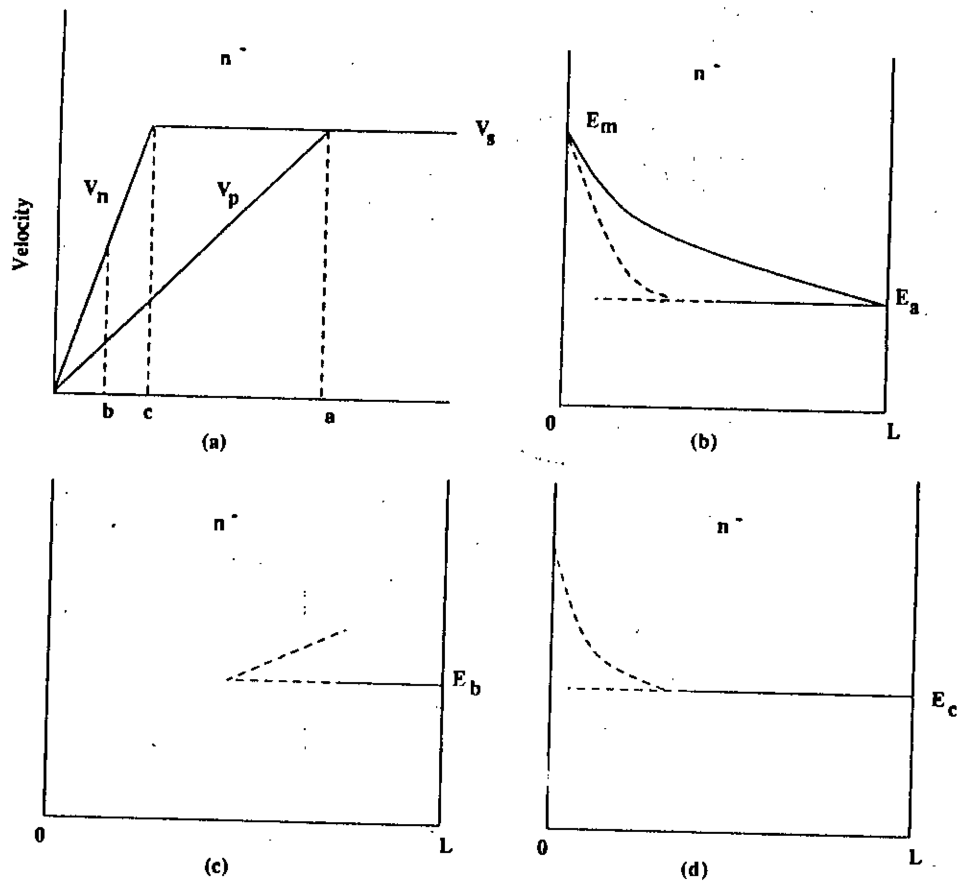

Fig.2.3. (a) Idealized velocity-field charactersitics for holes and electrons. E_a= field at a, E_b= field at b, E_c = field at c.

(b) If E_a is the field at the base region then any change in E does not change electron or hole densities so that $\frac{dE}{dx}$ remains zero.

(c) If E_b is the field at the base region then any increase in E implies that $\frac{dE}{dx}$ becomes positive - a total contradiction of the requirement that $\frac{dE}{dx}$ is negative.

(d) With E_c at the base, any change in E gives a negative $\frac{dE}{dx}$ and the field grows rapidly to a high value where avalanche injection starts.

$\frac{dE}{dx}$ would then be positive as one moves towards the collector contact in total contradiction of the requirement that $\frac{dE}{dx}$ is negative (with the sign convention for x that is used in Fig.2.3).

Fig.2.3(d) shows an ideal situation where electrons will be in a field E_C, just moving with their saturated velocity. If the electric field increases, their velocity and density do not change. The hole density is reduced-because the holes move faster but the hole current remains the same. A small change will produce a large change in carrier concentration. This change helps in further increase of the electric field and the field will grow fast to reach the condition where both holes and electrons move at their saturated velocities and varies linearly until it attains a value where avalanche multiplication starts.

However, the low field E_C adjacent to the base can be even lower if out-diffusion of holes from the base is permitted. The above discussion can be summed up by Fig.2.4. The scenario is that the minimum electric field at the collector edge of the base-collector junction is E_C and at this field a quasi-neutral region will exist.

So far the volt-ampere characteristics, electric field profile

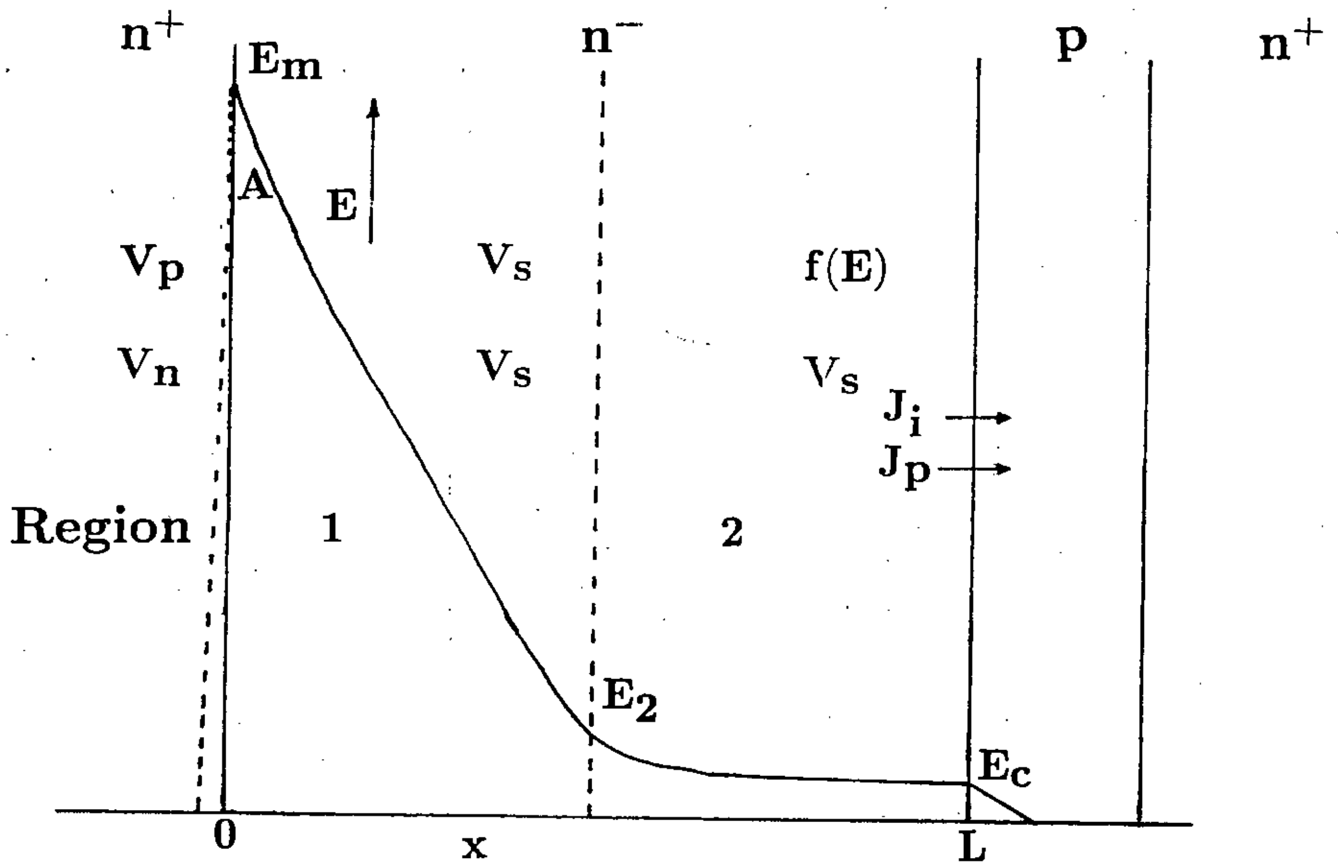

Fig.2.4. Field profile for CSB. with an extended low field region. J_p is the returned hole current from ionization caused by the injected electron current J_i. A marks the avalanche zone.

and velocity profile were given for reverse bias current mode second breakdown for transistors. The same analysis can be extended for open-base condition with some modifications.

The zero-base current or open-base condition appears then to correspond to the theory with the greatest length of neutral region (i.e. the longest plasma region) where recombination would be greatest.

If the base contact is such that it is biased so that holes cannot escape, then the returning hole current, generated by the avalanche region, must accumulate holes until these can recombine with the electrons at the same rate as they are generated. Fig.2.5 shows this schematically with a recombination zone adjacent to the base absorbing all the holes produced by the avalanche zone. The field profile, shown in fig 2.5 is similar to those shown before except the region of recombination close to the base. Within this recombination region, the electric field is suppressed to a very low value due to the accumulation of high hole and electron concentrations. However, the emitter-base voltage now has to be strongly positive so as to drive enough recombination electron current into the device. Thus, with $I_b = 0$, the base-emitter voltage is forward biased though because of the high currents and base resistance this voltage is well above the normal value of 0.7 V

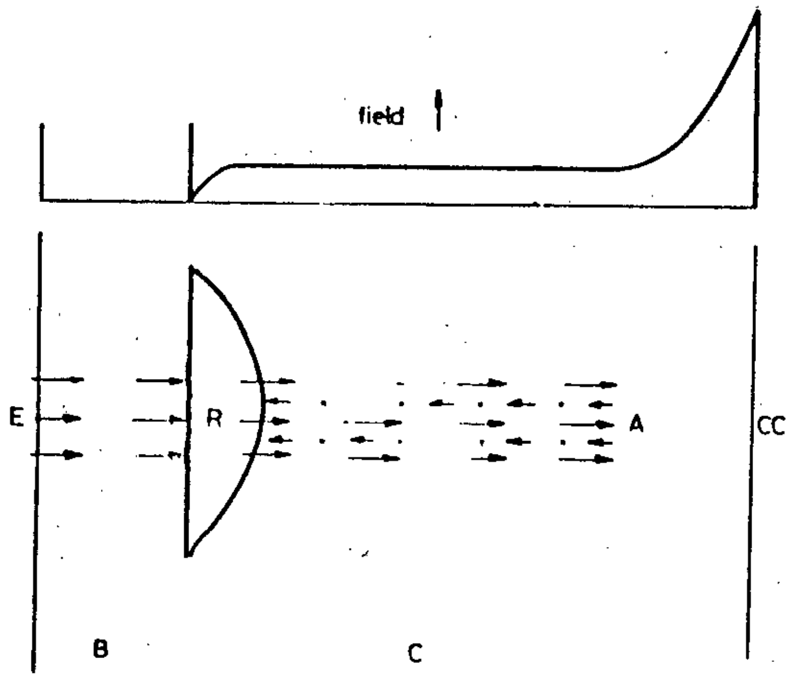

Fig.2.5. Schematic diagram for second breakdown with strong recombination.
electron
hole

for a forward biased Si p-n junction. The electric field in the base collector region are then similar to those in the Kirk effect. Thus, second breakdown and Kirk effect merge into one another. Second breakdown is complete when the avalanche zone has to supply all the hole recombination current. The Kirk effect is complete when the base supplies all the hole recombination current. Under the condition $I_b=0$, there is no external current flowing along the base region to force the emitter current into the centre of the emitter stripe and the emission is confined to the edges of the emitter.

2.3. Analytical Expression for Multiplication Factor of Transistor Driven in CSB

To estimate the collector-base voltage for the extended low field region of Fig.2.3(d) it is required to find out the boundary conditions on the hole and electron currents as well as the current multiplication factor M_n.

The Poisson's equation is,

$$\epsilon \frac{dE}{dx} = q\ (p+N_{DC}-n) \qquad (2-2)$$

In the extended low field region $\frac{dE}{dx} \approx 0$ and the electric field was chosen E_C at which $V_p = V_s/3$ (9) for S_i at $E=2\times10^4$ V/cm from Fig.2.3(a).Then,

$$\frac{J_p}{v_p} + \frac{J_o}{v_s} - \frac{J_N}{v_s} = 0 \qquad (2\text{-}3)$$

Hence at $E = E_C$, $J_n = J_{ns}$ (injected electron current) and $J_p = J_{ps}$ (current due to returning holes). Then,

$$3\ J_{ps} + J_o - J_{ns} = 0 \qquad (2\text{-}4)$$

Again with $J_n + J_p = J_{ns} + J_{ps} = J$,

current multiplication factor $M_n = \frac{J}{J_n}$

and above boundary conditions, eqn.(2-4) can be solved to find out M_n as follows,

$$\frac{J}{M_n} - J_o - 3J\left(\frac{M_n - 1}{M_n}\right) = 0 \qquad (2\text{-}5)$$

$$M_n = \frac{4J}{3J + J_o} = \frac{4P}{3P + 1} \qquad (2\text{-}6)$$

where $P = J/J_o$

When the transistor goes into CSB, current density will be very large and M_n increases to 4/3.

2.4. Numerical Solution

It is difficult to obtain an exact solution of the avalanche injection problem. However, electric field and current density in the high field collector region can be obtained from one dimensional analysis using the following assumptions,

(1) Recombination is negligible for high field region.

(2) Consideration of only the drift component of the

current within high field zone.

(3) Electron and hole saturated velocities are equal.

The diffusion component is important only at low electric field. Since the electric field, which is beyond the onset of saturation is dealt with in this analysis, neglecting the effect of diffusion in determining the electric field and current density, is justified.

The main objective of this thesis is to find an analytical solution for collector voltage under CSB. The analytical equation for electric field for avalanche injection zone is obtained with some assumptions. To justify the assumptions, the results need to be compared with numerical values. For this reason, the electric field distribution and voltage for avalanche injection region are computed numerically. In chapter 3, it has been shown that the results are in good agreement with numerical values. Now the required portion of the collector is divided into two regions [Fig.2.4]. In region I, there is no carrier generation. In region II, avalanche generation occurs which increases the electric field gradient.

The basic equations to be solved are:

$$J = J_n + J_p = qV_n n + q\, V_p p \qquad (2\text{-}7)$$

$$\epsilon \frac{dE}{dx} = q(n - N_{DC} - p) \qquad (2\text{-}8)$$

$$J_n = \frac{J}{M_n} = \frac{3J + J_o}{4} \qquad (2\text{-}9)$$

$$\frac{dJ_n}{dx} = -\frac{dJ_p}{dx} = \alpha J_n + \beta J_p \qquad (2\text{-}10)$$

The final eqns. to be solved numerically are,

$$\frac{dE}{dx} = \frac{1}{\epsilon v_s}(2J_n(x) - J_o - J) \qquad (2\text{-}11)$$

$$\frac{dJ_n}{dx} = (\alpha - \beta)J_n + \beta J \qquad (2\text{-}12)$$

where $\alpha = A_n \exp - B_n / E cm^{-1}$

$\beta = A_h \exp - B_h / E cm^{-1}$

2.4.1. Boundary Values of Electric Field

The boundary conditions are:

at $x = 0$, $E = 6 \times 10^4$ V/cm

at the collector-substrate interface $J = J_n$ and $J_p = 0$.

Since the collector-substrate is heavily doped, $p = 0$.

2.4.2. Numerical Techniques used in Computation of Electric Field and Current Density

With the boundary conditions mentioned in section 2.4.1, equation (2.11) and (2.12) can be solved numerically. Here, Runge-Kutta initial value method is applied for computation of electric field distribution and current density within the high field collector region. The area under the field distribution will give the voltage across the high field region. When $J>J_o$, the maximum electric field will occur at the collector-substrate interface (n^-n^+) where the current density will consist of electron current only as the hole current is zero at the interface. For a given J, J_n at the point where $E = 6x10^4$ V/cm can be calculated from the eqn.,

$$J_n = J/M_n \qquad (2\text{-}13)$$

With this J and J_n as boundary values, the field distribution for the high field region can be obtained by using Runge-Kutta 4 point initial value method.

The electron and hole current densities as a function of distance are shown in Fig.2.6, whereas Fig.2.7 is plotted with electric field as a function of distance for several current densities for a given collector doping density, $N_{DC}=2x10^{15}$ cm^{-3}.

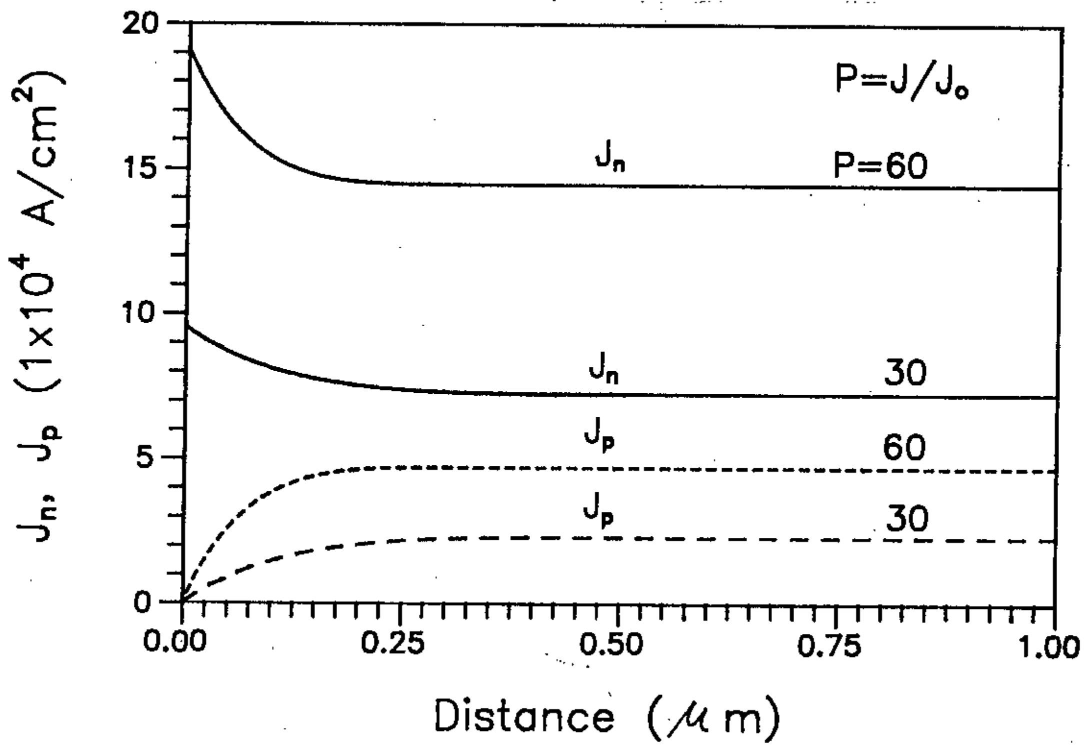

Fig.2.6. Electron and hole current density as a function of distance.

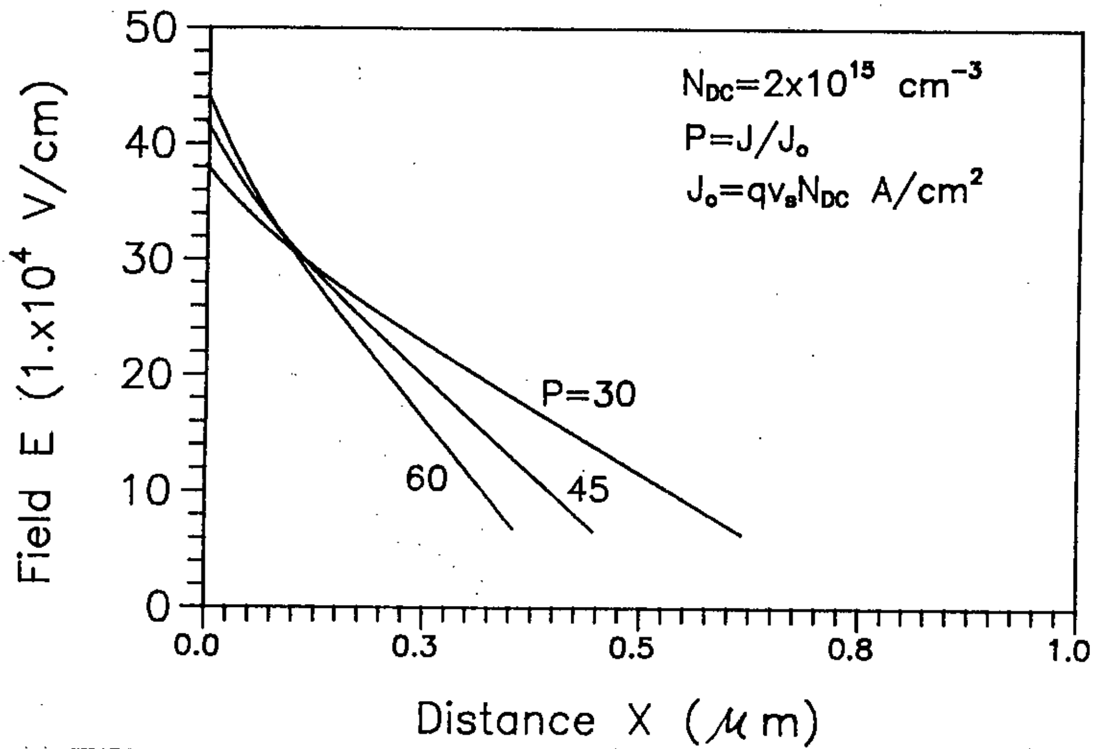

Fig.2.7. Field distribution for various current densities.

2.4.3. Features of Numerical Results

From the plots drawn in section 2.4.2, certain conclusions can be drawn:

(1) From Fig.2.6, it can be seen that $J_n(x)$ and $J_p(x)$ vary sharply in a narrow region. In this region the carrier multiplication factors α and β becomes very large. The region in which J_n and J_p vary is known as the multiplication region.

(2) In the region (Fig.2.7) where electron and hole velocities are saturated but the carrier generation is negligible, the field is essentially linear with position. This region contributes substantially to the total voltage drop across the collector region. As J increases, the area under this region decreases, and this contributes to the negative resistance behavior in the avalanche injection situation.

(3) From Fig.2.7, it is clear that in the multiplication region the field departs from linearity. Therefore, the boundary of this region should be accurately identified as the point where generation creates a disturbance on the charge density, rather than the point where the field reaches a critical value. In the next chapter, based on the above observations, an analytical model is developed for CSB, using the regional approximation method.

2.5. Conclusions

The numerical analysis developed in this chapter for high field region has pointed out the role of the injection of carriers from the collector-substrate interface and the velocity saturation in the negative resistance of the device. The region where both electron and hole velocities are saturated but the carrier generation is negligible plays the most important role in lowering the terminal voltage. In the next chapter, analytical model is developed on the basis of the important features of the numerical analysis.

CHAPTER 3

Analytical Solution

3.1. Introduction

When a transistor drives into current mode second breakdown, its terminal voltage decreases to a low value. This low voltage is called the holding voltage. To estimate this voltage, a linear-approximation method is applied. The whole collector region is divided into six zones. Analytical expression for each of these regions is derived. Analytically obtained field distributions within avalanche injection zone is compared with the numerically obtained field distributions. Both the distributions match well.

3.2 Analysis

The analysis is carried out for an $n^+pn^-n^+$ transistor (shown in Fig.3.1) with the collector base metallurgical junction taken as the origin. To derive equations to describe current mode second breakdown, in this work, the epitaxial layer(collector) is divided into six regions (Fig.3.2). The zones are chosen with the consideration of changes in mobility, quasi-neutrality, generation and recombination of carriers. There are six basic equations which leads to this analysis, these are,

$$J = J_n + J_p \qquad (3\text{-}1)$$

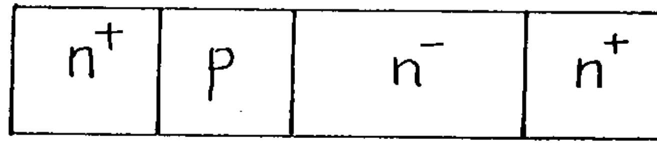

Fig.3.1. An $n^+pn^-n^+$ structure.

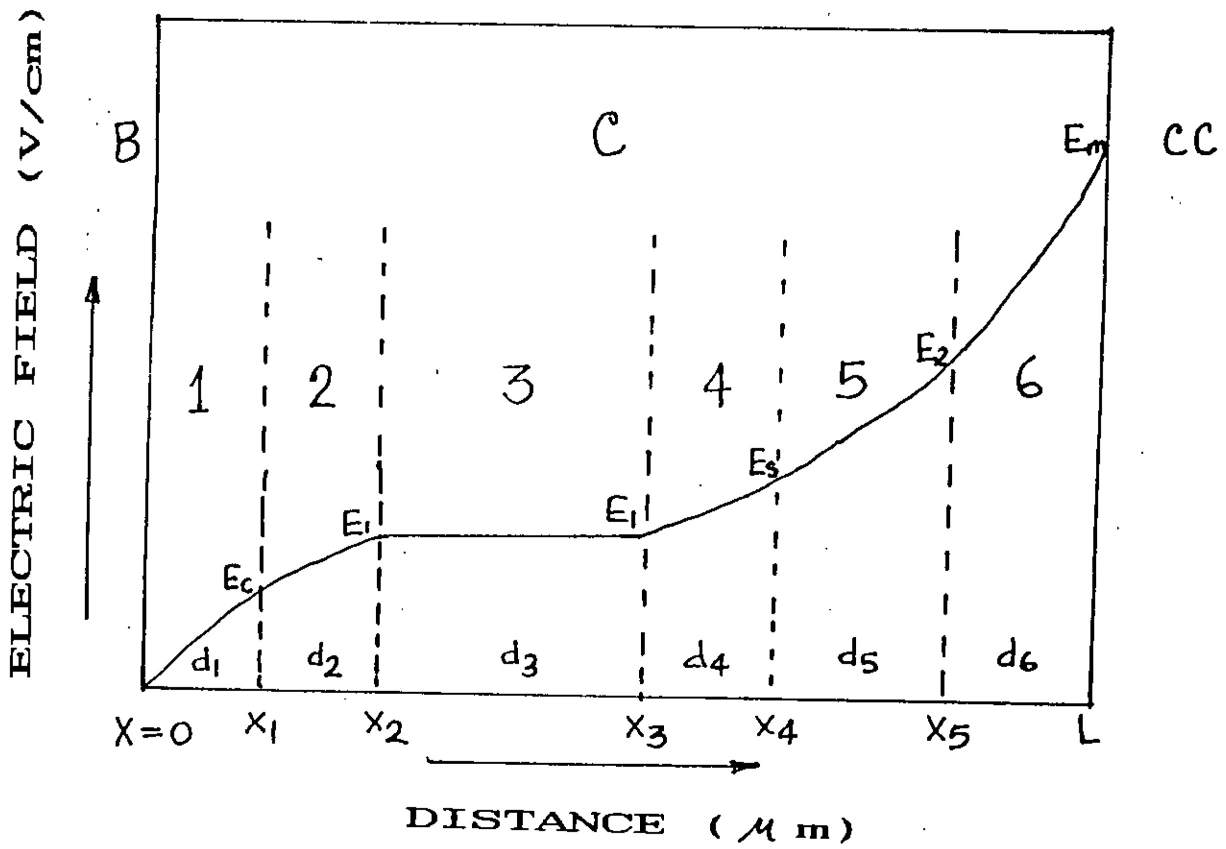

Fig.3.2. Electric field profile in the collector region.

$$J_n = qv_n n - qD_n \frac{dn}{dx} \tag{3-2}$$

$$J_p = qv_p p + qD_p \frac{dp}{dx} \tag{3-3}$$

$$\frac{1}{q}\frac{dJ_n}{dx} = g - r \tag{3-4}$$

$$-\frac{1}{q}\frac{dJ_p}{dx} = g - r \tag{3-5}$$

$$\frac{dE}{dx} = \frac{q}{\epsilon}(n - N_{DC} - p) \tag{3-6}$$

where

$$g = \frac{1}{q}(\alpha J_n + \beta J_p)$$

The generation of carriers by avalanche multiplication requires a large electric field. Since avalanche injection occurs at the n^-n^+ interface, the electric field increases towards the n^-n^+ interface and attains its maximum value, which must exceed the saturation value E_s = 6 x 10^4 V/cm. Starting from the collector base metallurgical junction, the first region is characterized by charge neutrality with very low electric field. The second region is characterized by tepid electron regime. The third has quasi-neutrality with constant electric field E_1. The fourth region has constant electron density and constant electron velocity. The fifth region is characterized by constant hole and

electron carrier densities with negligible avalanche ionization, which in turn dominates the sixth region near n^-n^+ interface. In detail, the six regions are characterized as follows :

3.2.1. REGION 1 ($0 < x < x_1$)

Electrons injected from the E-B junction enter this region through the base; holes generated from the avalanche injection zone enter this volume leading to a conductivity modulated region which is almost neutral and has low field.

Eqns. (3-2) and (3-3) can be rewritten after differentiating w.r.t.x,

$$\frac{dJ_n}{dx} = q\mu_n \frac{d}{dx}(nE) - qD_n \frac{d^2 n}{d^2 x} \qquad (3\text{-}7)$$

$$\frac{dJ_p}{dx} = q\mu_p \frac{d}{dx}(pE) + qD_p \frac{d^2 p}{d^2 x} \qquad (3\text{-}8)$$

Substituting $b = \frac{\mu_p}{\mu_n}$ and $\frac{D_n}{\mu_n} = \frac{D_p}{\mu_p} = \frac{kT}{q} = V_t$

eqns. (3-7) and (3-8) can be written as,

$$-\frac{b}{q}\frac{dJ_n}{dx} = -\mu_p \frac{d(nE)}{dx} + \mu_p V_t \frac{d^2 n}{dx^2} \qquad (3\text{-}9)$$

$$\frac{1}{q}\frac{dJ_p}{dx} = \mu_p \frac{d(pE)}{dx} + \mu_p V_t \frac{d^2 p}{dx^2} \qquad (3\text{-}10)$$

Solving eqns. (3-9) and (3-10),

$$\frac{1}{q}\left[\frac{dJ_P}{dx} - b\frac{dJ_n}{dx}\right] = \mu_p \frac{d}{dx}[(p-n)E] + \mu_p V_t \frac{d^2}{dx^2}(p+n) \qquad (3\text{-}11)$$

If generation is neglected then by combining eqns.(3-4),(3-5) and (3-11), the following equation can be obtained,

$$\frac{r(b+1)}{\mu_p} = \frac{d(p-n)E}{dx} + V_t \frac{d^2}{dx^2}(p+n) \qquad (3\text{-}12)$$

Using eqn.(3-6), eqn. (3-12) can be written as,

$$V_t \frac{d^2}{dx^2}(p+n) - N_{DC}\frac{dE}{dx} - \frac{\epsilon}{q}\frac{d}{dx}\left(E\frac{dE}{dx}\right) = \frac{r(b+1)}{\mu_p} \qquad (3\text{-}13)$$

The solution to equation (3-13) is in general extremely complicated, however, it has been demonstrated by Schilling and Lampert [11] on the basis of the numerical solutions obtained by Baron [12], that the third term in (3-13) can be safely neglected; furthermore in the vicinity of the collector side of the collector-base junction, the electric field varies slowly due to the quasi-neutrality condition.

So it can be written,

$$n - p - N_{DC} = 0 \qquad (3\text{-}14)$$

$$\Rightarrow p + n = 2p + N_{DC} \qquad (3\text{-}15)$$

With this assumption, eqn. (3-13) becomes,

$$2V_t \frac{d^2 p}{dx^2} - N_{DC}\frac{dE}{dx} = \frac{r(1+b)}{\mu_p} \qquad (3\text{-}16)$$

The first term of L.H.S of equation (3-16) is due to diffusion and the second term is due to drift.

Since P>> N_{DC} in this volume, N_{DC} can safely be neglected. Again, recombination $r = \frac{p - p_p o}{\tau_p} \approx \frac{p}{\tau_p}$ since P>>P_{po}. Then (3-16) can be rewritten as,

$$2V_t \frac{d^2 P}{dx^2} = \frac{r(b+1)}{\mu_p} \tag{3-17}$$

To solve the eqn.(3-17), the following boundary conditions will be used,

at $x = 0$, $p = p_o$

at $x = x_1$, $p = p_s$

With this boundary values, the solution of eqn. (3-17) can be written as,

$$p(x) = \frac{\left(p_s - p_o Cos\frac{x_1}{L_a}\right)}{Sin\frac{x_1}{L_a}} Sin\frac{x}{L_a} + p_o Cos\frac{x}{L_a} \tag{3-18}$$

Where $L_a = \sqrt{\left(\frac{2V_t \mu_p \tau_p}{1+b}\right)}$

Actually, at $x=x_1$, a transition from the cold electron regime of the first region to the hot electron regime of the second region occurs. The neutrality condition (3-14) does not hold all along the collector region because the avalanche injection regime

requires also the existence of a space charge region with saturated drift velocity.

For $x_1 < L_a$, $\mathrm{Sin}(x_1/L_a) = x_1/L_a$ and $\mathrm{Cos}(x_1/L_a) = 1$

Thus it is found,

$$p(x) = \frac{p_s - p_o}{x_1} x + p_o \tag{3-19}$$

So a linear relationship of hole with respect to distance x is observed. At this moment the expression of current density J will be derived to find out Electric field E.

The current equation is,

$$J = J_n + J_p$$

$$= q\mu_n E\left(N_{DC} + (1+b)p\right) + qV_t\mu_n(b-1)\frac{dp}{dx} \tag{3-20}$$

The electric field is,

$$E = \frac{\dfrac{J}{q\mu_n} - V_t(b-1)\dfrac{dp}{dx}}{p(1+b) + N_{DC}} \tag{3-21}$$

Since, $E = E_c$, at $x = x_1$

and $p = p_s$

Then eqn. (3-21) becomes,

$$E_C = \frac{\dfrac{J}{q\mu_n} - V_t(b-1)\dfrac{p_o - p_s}{x_1}}{p(1+b) + N_{DC}} \tag{3-22}$$

In equation (3-22), there are three unknowns; p_o, x_1, p_s. So two more equations are needed to find out the unknowns.

The recombination current is,

$$J_r = \frac{q}{\tau_p}\int_0^{x_1} p(x)dx \qquad (3\text{-}23)$$

With the help of eqn. (3-19), J_r can also be written as,

$$J_r = \frac{q}{2\tau_p}(p_i + p_o)x_1 \qquad (3\text{-}24)$$

Current multiplication factor $M_n = J/J_{ns}$ (3-25)

$$J = J_{ns} + J_{ps} \qquad (3\text{-}26)$$

From equations (3-25) and (3-26),

$$J_{ps} = (M_n - 1)J_{ns} \qquad (3\text{-}27)$$

The recombination current is found from the equation of hole current entering into this volume from region 2,

$J_{ps} = J_r + AJ_{ni}$ (3-28)

Where, $A = J_{pi}/J_{ni}$ and

$$J = J_{ni} + AJ_{ni} \tag{3-29}$$

$$J_{ni} = \frac{M_n}{1+A} J_{ns} \tag{3-30}$$

From eqns. (3-27), (3-28) and (3-30), it can be shown that,

$$J_r = \left(\frac{M_n}{1+A} - 1\right) \frac{J}{M_n} \tag{3-31}$$

J_{ns} in equation (3-27) is the electron current density entering the hot electron regime (region 2) where recombination has been neglected and J_{ni} in equation (3-28) is the electron current density entering this volume from the base.

J_r exists when $A < (M_n - 1)$.

Again at $x = x_1$, $J_p = J_{ps}$, neglecting recombination, J_{ps} can be obtained as,

$$J_{ps} = qv_p p_s = (M_n - 1) J_{ns} = \frac{M_n - 1}{M_n} J \tag{3-32}$$

With $v_p = v_s/3$ [10] when $E = E_1 = 2 \times 10^4$ V/cm

$$p_s = 3 \frac{M_n - 1}{M_n} \frac{J}{qv_s} \tag{3-33}$$

In equation (3-31), where A is unknown, however, a value can be assumed and justified.

$A = 1 - \alpha = 1 - .999 = .001 = 10^{-3}$ or 2×10^{-3} and that does not matter so far (1+A) is concerned.

For a given J, M_n can be calculated from eqn(2-6) and with this J and M_n, p_s is known from equation (3-33). J_r will be known if A is known. With these values of J_r and p_s, x_1 and p_o can be determined easily from equations (3-22), (3-24) and (3-31) for a given J.

The voltage in the low field region is given by,

$$V_1 = \int_0^{Ec} E(x)dx \qquad (3\text{-}34)$$

Assuming $N_{DC} \ll p$, and from eqns. (3-19) and (3-21), the final form of the voltage in the first region can be written as,

$$V_1 = \frac{Qx_1}{p_o - p_s} ln \frac{p_o}{p_s} \qquad (3\text{-}35)$$

where,
$$Q = \frac{\frac{J}{q\mu_n} + \frac{V_t(b-1)}{x_1}(p_o - p_s)}{1+b} \qquad (3\text{-}36)$$

From the equations (3-24) and (3-31), the final expression of the distance can be written as,

$$x_1 = \frac{J - J_o}{p_s - p_o}\frac{\tau_p}{2q} \qquad (3\text{-}37)$$

For a given J, X_1 can be calculated if P_o and P_s are known.

3.2.2. REGION 2 ($x_1 < x < x_2$)

In this region E > 2 x 10^3 V/cm. The basic assumptions for this region are:

(1) diffusion term can be neglected.

(2) generation and recombination terms are neglected so that J_p takes the constant value J_{ps}, entering from the third region.

(3) in Poisson's equation, the excess hole density is neglected with respect to the density p_s, entering from the third region. However, this region effects only slightly the J-V characteristics at high current densities. So these assumptions lead to small error. From the velocity-field curve, the velocity of hole and electron can be found out for region II.

For $E < 2 \times 10^3$ V/cm, assuming the velocity linearly varies with E in this region,

$$v_n = \mu_n E = 1500\ E \tag{3-38}$$

$$v_p = \mu_p E = 600\ E \tag{3-39}$$

For region II where $2\times10^3 < E < 2\times10^4$ V/cm,

$$v_p = \mu_p E + v_{po} \tag{3-40}$$

$$v_n = \mu_n E + v_{no} \tag{3-41}$$

With the help of eqn.(3-38) and (3-39),

at $E = E_C$, $v_n = 3\times10^6$ cm/s

$v_p = 1.2\times10^5$ cm/s

at $E = E_1$, $v_n = v_p = 10^7$ cm/s.

Then from eqns.(3-40) and (3-41),

$v_{no} = 22.2\times10^5$ cm/s

$\mu_n = 389$ cm^2/V-s

$v_{po} = 8.9\times10^5$ cm/s

$\mu_p = 152$ cm^2/V-s

Now from eqn.(3-6),

$$\frac{dE}{dx} = \frac{1}{\epsilon}\left[\frac{J_{ns}}{v_s} - \frac{J_{ps}}{v_p} - \frac{J_o}{v_s}\right] \tag{3-42}$$

With the help of eqn.(3-40) and (3-41), the following eqn. is formed,

$$\frac{dE}{dx} = \frac{A}{\mu_n E + v_{no}} - B \tag{3-43}$$

where $A = \frac{J_{ns}}{\epsilon}$ and $B = \frac{1}{\epsilon_s}\left(\frac{J_{ps}}{v_p} + \frac{J_o}{v_s}\right)$

Solving eqn.(3-43) for electric field within the region II, the following equation is found,

$$-\frac{1}{B}(E - E_C) + \frac{A}{B^2\mu_n} ln\left(\frac{\frac{A - v_{no}B}{\mu_n} - E}{\frac{A - v_{no}B}{\mu_n} - E_C}\right) = x - x_1 \tag{3-44}$$

At $x = x_2$, $E = E_1$, then the distance in this region is,

$$d_2 = \frac{A}{B^2\mu_n} ln\left(\frac{\frac{A - v_{no}B}{\mu_n B} - E_1}{\frac{A - v_{no}B}{\mu_n B} - E_C}\right) - \frac{1}{B}(E_1 - E_C) \tag{3-45}$$

The voltage developed across the region is,

$$V_2 = \int_{E_C}^{E_1} E dx \tag{3-46}$$

With the help of eqn.(3-45), the final form of eqn.(3-46) becomes,

$$V_2 = -\frac{1}{2B}(E_1^2 - E_C^2) - \frac{A}{\mu_n B^2}(E_1 - E_C) + \frac{A(A - v_{no}B)}{\mu_n^2 B^3} \quad ln \left(\frac{\frac{A - v_{no}B}{\mu_n B} - E}{\frac{A - v_{no}B}{\mu_n B} - E_C} \right) \tag{3.47}$$

3.2.3. Region 3 ($x_2 < x < x_3$)

In this region only electrons move with saturated velocity and net charge density is zero and quasi-neutrality exists in this region. Electric field is almost constant i.e. gradient of electric field is zero.

Mathematically,

$$\epsilon \frac{dE}{dx} = q(p + N_{DC} - n) \approx 0 \tag{3-48}$$

So E is constant and $E = E_1 = 2 \times 10^4$ V/cm.

The thickness of this volume d_3 can be calculated when the widths of other regions are known. The voltage of region 3 can be written as,

$$V_3 = \int_{x_2}^{x_3} E.dx = E_1 d_3 = E_1(x_3 - x_2) \tag{3-49}$$

At high current densities, the space charge limited region (region 4,5,6) decreases to a small value and this region extends towards the C-B metallurgical junction. On the otherhand, the recombination zone extends towards the n^-n^+ contact with the increase of J.

3.2.4. Region 4 ($x_3 < x < x_4$)

In this region, only electrons move with their saturated velocity. This region terminates where the electric field is equal to E_s and both electrons and holes move with saturated velocity. Electron entering into this region will reach the avalanche zone without any recombination. Holes generated in the avalanche zone will first enter region 5 (where both electrons and holes move with saturated velocity) and then enter the region 4 where the electric field decreases to a value E_s and holes move with a field dependent velocity. Space charge limited current will flow throughout this region.

The voltage and electric field can be calculated from eqn.(3-6) by choosing appropriate boundary conditions.
In this region $2x10^4 < E < 6x10^4$ V/cm.

From eqn.(3-6) and writing $J_n = J_{ns}$ and $J_p = J_{ps}$, it can be written ,

$$\epsilon \frac{dE}{dx} = \frac{J_{ns}}{v_s} - \frac{J_{ps}}{\mu_{pE}} - \frac{J_o}{v_s} \qquad (3\text{-}50)$$

With the help of eqns.(3-25), (3-26) and (3-27), eqn.(3-50) becomes,

$$\frac{dE}{dx} = B - \frac{A}{E} \qquad (3\text{-}51)$$

where
$$A = \frac{J}{\epsilon \mu_p}\left(1 - \frac{1}{M_n}\right) \qquad (3\text{-}52)$$

$$B = \frac{1}{\epsilon v_s}\left(\frac{J}{M_n} - J_o\right) \qquad (3\text{-}53)$$

Now, eqn.(3-51) can be solved easily to find the electric field by the following equation,

$$x = \frac{E}{B} + \frac{a}{B^2} ln\left(E - \frac{A}{B}\right) + C \qquad (3\text{-}54)$$

where C is an arbitrary constant.

The voltage in the region 4 is found from the following expression,

$$V_4 = \int_{x_3}^{x_4} E.dx \qquad (3\text{-}55)$$

Solving eqn.(3-55) with the help of eqn.(3-54), the eqn of voltage is obtained,

$$V_4 = \frac{E_s^2 - E_3^2}{2B} + \frac{A}{B^2}(E_s - E_3) + \frac{A^2}{B^3} ln \frac{E_s - \frac{A}{B}}{E_3 - \frac{A}{B}} \tag{3-56}$$

The distance d_4 is found from the eqn.(3-54) with appropriate boundary conditions and can be expressed as,

$$d_4 = (x_4 - x_3) = \frac{E_s - E_3}{B} + \frac{A}{B^2} ln \frac{E_s - \frac{A}{B}}{E_3 - \frac{A}{B}} \tag{3-57}$$

3.2.5. Region 5 ($x_4 < x < x_5$)

Electron and hole velocities are both saturated in this region but the carrier generation can be neglected. So a linear relationship exists for electric field and is given by,

$$E(x) = E_s(x) + \frac{dE}{dx}(x - x_4) \tag{3-58}$$

Then from eqn. (3-1) and (3-6), it can be written that,

$$\epsilon \frac{dE}{dx} = \frac{2J_n - J_o - J}{v_s} \tag{3-59}$$

At $x = x_4$, substituting the value of M_n from eqn. (2-4), the slope of the field is found as,

$$\frac{dE}{dx} = \frac{J - J_o}{2\epsilon v_s} \quad (3\text{-}60)$$

With the help of eqn. (3-60), eqn. (3-58) can be rewritten as,

$$E(x) = E_s(x) + \frac{J - J_o}{2\epsilon v_s}(x - x_4) \quad (3\text{-}61)$$

The fifth region is terminated where the generation of carriers can no longer be neglected and the generation in region 6 gives rise to a disturbance in the existing charge density in region 5. Due to this reason as one approaches towards region 6, the change in slope of the electric field occurs. The boundary x_5 is taken as the point where the disturbance in charge density gives a slope equal to the average of the two slopes,
one with $J_p = 0$ at $x = L$ and the other with constant J_n and J_p. Thus,

$$\frac{dE}{dx} = \frac{J - J_o}{\epsilon v_s} \quad (3\text{-}62)$$

Again, integrating eqn.(3-4) and (3-5), it can be written,

$$J_n(x) = J_{ns} + \int_{x_4}^{x} g\,dx \quad (3\text{-}63)$$

$$J_p(x) = J_{ps} + \int_{x_4}^{x} g dx \tag{3-64}$$

Where the generation rate,

$$g = \alpha J_n(x) + \beta J_p(x) \tag{3-65}$$

And $J_{ns} = J_n(x_4)$ and $J_{ps} = J_p(x_4)$.

Solving eqn. (3-6) with the help of eqns. (3-63), (3-64) and (3-65), the following eqn. for slope of electric field at any x is obtained,

$$\frac{dE}{dx} = \frac{1}{2\epsilon v_s}(J - J_o) + \frac{2}{\epsilon v_s}\int_{x_4}^{x} g dx \tag{3-66}$$

The value of slope of electric field at $x = x_5$ is equal to the average of two slopes found by eqns. (3-60) and (3-62). Thus,

$$\text{Average slope} \quad S_{av} = \frac{dE}{dx} = \frac{3(J - J_o)}{4\epsilon v_s} \tag{3-67}$$

Now this average slope of eqn. (3-67) and the slope found in eqn. (3-66) will intersect at a point and by equating them, the following eqn. is obtained,

$$\int_{x_4}^{x_5} g dx = \frac{J - J_o}{8} \tag{3-68}$$

The left side of the above equation can be solved with some

approximations with the help of eqn.(3-65) (Appendix A) and the solution determines the electric field E_2,

$$E_2^2\left(\frac{a_n}{b_n}\exp-\frac{a_n}{E_2}+\frac{a_n}{b_n}(M_n-1)\exp-\frac{b_h}{E_2}\right)=\frac{M_n}{16\epsilon v_s J}(J-J_0)^2 \qquad (3\text{-}69)$$

A comparison between the numerical and analytical results is shown in Fig. 3.3 and it is found that with this approximation for the slope, the error introduced is small.

The distance d_5 is found by dividing the difference of electric field across the region by the slope found in eqn. (3-60) and is given by,

$$d_5=\frac{2\epsilon v_s}{J-J_o}(\ E_2-E_s\ ) \qquad (3\text{-}70)$$

The voltage of region 5 is,

$$V_5 = \int_{x_4}^{x_5} E(x)\,dx \qquad (3\text{-}71)$$

With the help of eqn. (3-60), the final form of the voltage is

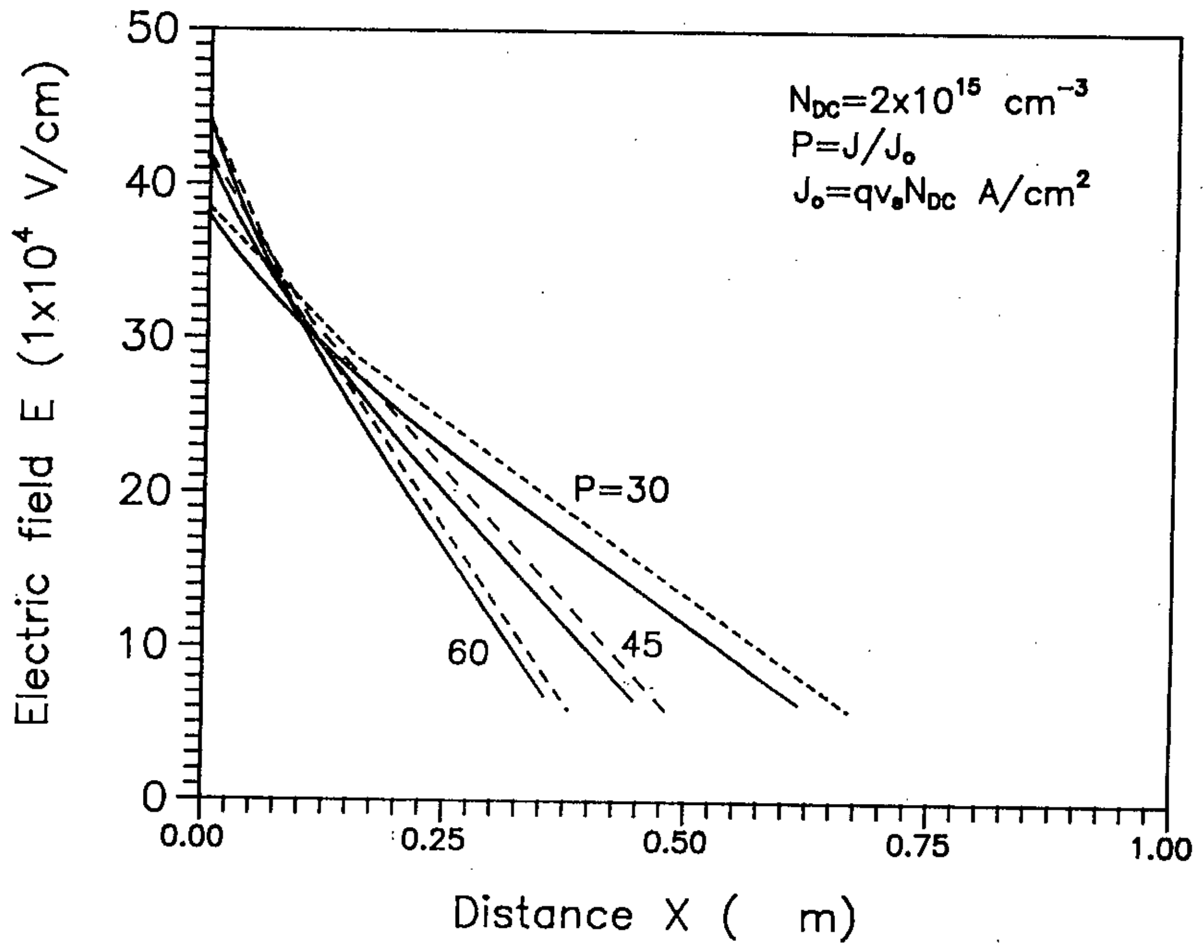

Fig.3.3. Comparison of analytically calculated field with numerical results
Solid line - numerically computed field.
Dashed line - analytically calculated field.

obtained,

$$V_5 = \frac{\epsilon v_s}{J - J_o}(E_2^2 - E_s^2) \qquad (3\text{-}72)$$

For $J >> J_o$,

$$V_5 \approx \frac{\epsilon v_s E_2^2}{J} \qquad (3\text{-}73)$$

This region plays a major role in lowering the device voltage because of the inverse relationship with J and decrease of width of the region.

3.2.6. Region 6 ($x_5 < x < L$)

Avalanche ionization dominates this region, causing the slope of the field to increase towards the contact. The numerical solution, however, suggests that the electric field distribution is nearly linear over the whole generation region (Fig.2.7). An analytical solution can be derived if the slope is assumed to be constant and taken as the average of the slopes at $x = L$ and $x = x_5$(in region 5 in absence of generation). This approximation yields eqn. (3-62) which can be reproduced as,

$$\frac{E_m - E_2}{L - x_5} = \frac{J - J_o}{\epsilon v_s} \qquad (3\text{-}74)$$

The width of region 6 is then given by ,

$$d_6 = \frac{E_m - E_2}{S_{av}} = \frac{4\epsilon v_s}{3(J - J_o)}(E_m - E_2) \qquad (3\text{-}75)$$

Where E_m = E(L) and E_2 = E (x_5). E_m and E_2 are related to the electron multiplication factor M_n and J (Appendices A and B).

The voltage drop in region 6 is then given by,

$$V_6 = \frac{2}{3}\frac{\epsilon v_s}{J - J_o}(E_m^2 - E_2^2) \qquad (3\text{-}76)$$

The avalanche ionization rate strongly depends upon the maximum electric field E_m. If J is increased by an order of magnitude, E_m increases only slightly. Therefore, Region 6 contributes a negative J-V characteristic. However, its contribution to the total voltage is not significant for the range of current densities that is dealt with. At high current density, the width of this region is very small and consequently the voltage drop in this region is small compared to the total voltage across the device.

The above analysis clearly shows that the voltage depends upon

epilayer thickness. Hence, this analysis explains the experimental observation [9] that the holding voltage depends upon collector length. The voltage across the collector is the sum of the voltage drops V_1, V_2, V_3, V_4, V_5 and V_6 in the six regions. The thickness of region 1,2,6 decreases as J increases. The region 3,4 and 5 are the main contributors to the negative resistance characteristics and are responsible for causing the experimentally observed low holding voltage.

J-V curves, obtained by this analytical model, are shown in Fig. 3.4. From the analytical expressions of voltages it is evident that at holding voltage the current is very high, much higher than J_o. Thus it can be concluded that holding voltage is independent of doping concentration but obviously depends on the epitaxial layer thickness. In Fig. 3.5, the dependence of holding voltage on epitaxial layer thickness is shown. It linearly varies with the thickness which was experimentally observed by Dunn and Nuttall [9]. Thus the results are in good agreement with the experimental observations.

3.3. Conclusions

The analytical model developed in this thesis explains the dependence of the holding voltage on the epitaxial layer thickness and estimates the holding voltage. It correctly

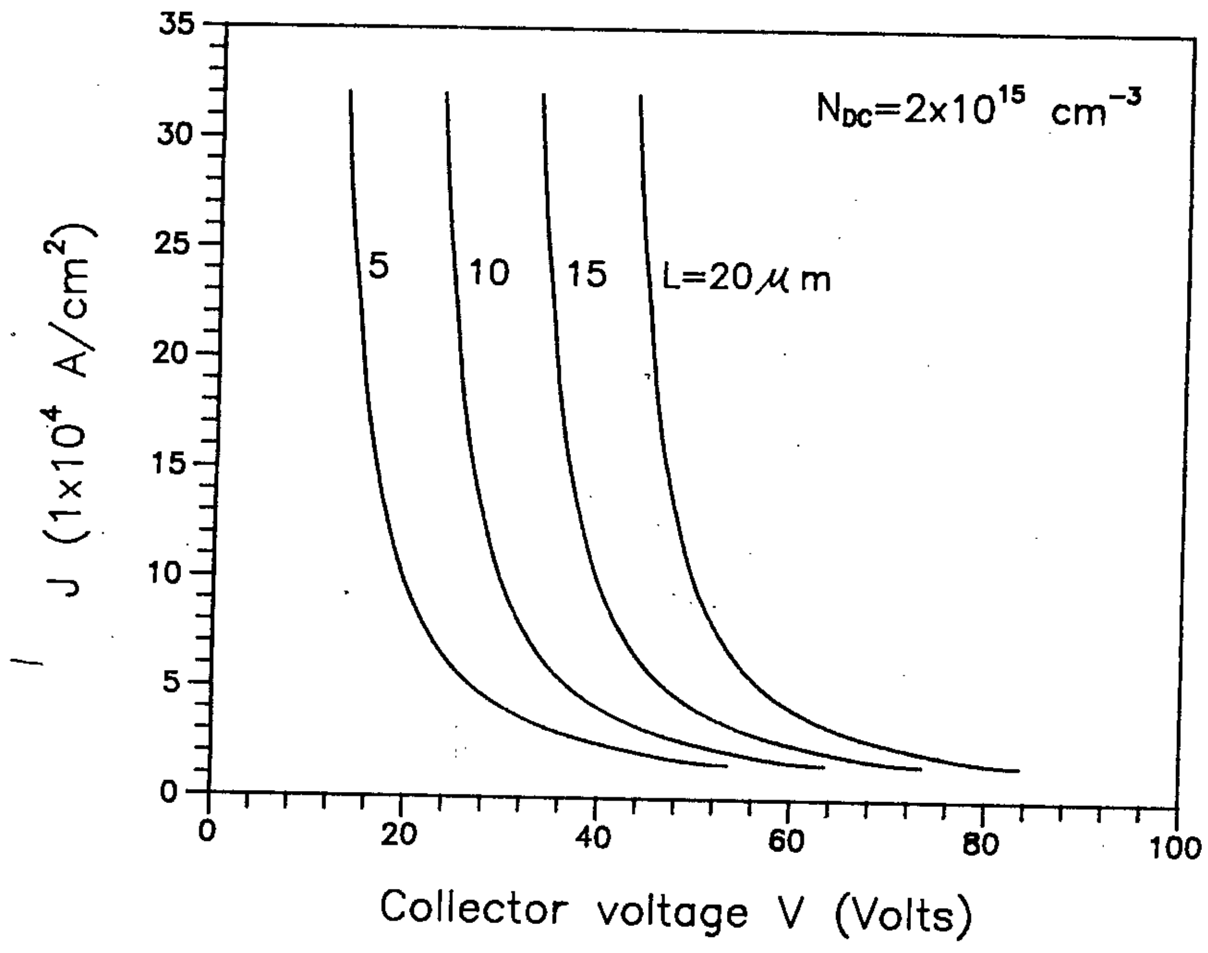

Fig.3.4. J-V characteristics for various epitaxial layer thickness.

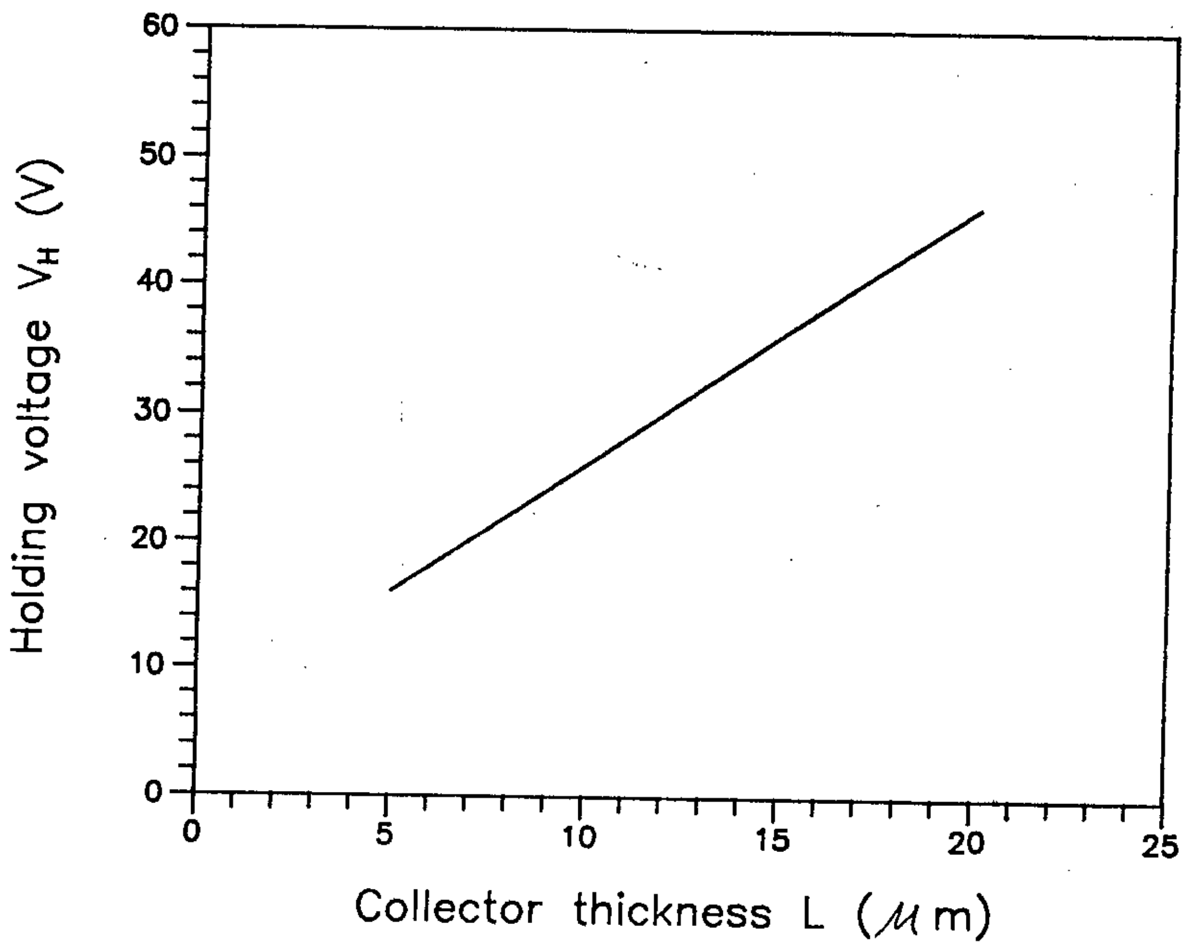

Fig.3.5. Holding voltage vs. epitaxial layer thickness curve.

predicts the role played by different regions of the bulk on the reduction of voltage when the transistor goes into current mode second breakdown. However, it is not possible to include the current spreading, a two-dimensional phenomena, in one dimensional model. This is the limitation of a one-dimensional model. The abrupt transition of the J-V characteristic is quite important from the standpoint of avoiding second breakdown in transistors. The power dissipated in the current mode second breakdown is related to this holding voltage and limits the time that a given device can survive in current mode second breakdown. Unless special circuit precautions are taken to limit the collector current, this current will increase and the device enters into thermal mode second breakdown with permanent damage.

CHAPTER 4

Conclusions

Devices that use transistor like structures with $n^+pn^-n^+$ layers when operated in an avalanche multiplication can be limited by current mode second breakdown. Under operation in steady state in reverse biased condition at high voltage any perturbation in voltage or current can switch this type of device from the normal active operational state into new states which are characterized by an increase in current and a reduction in voltage. The occurrence of this phenomenon can lead to a catastrophic failure of the device. For reliable operation of transistors with a widest range of safe operating conditions studies of current mode second breakdown are important. But, unfortunately, such studies are not easy because the transistor is often destroyed by the very effect one wishes to study. The field distortion with the collector arising from mobile space charge causes voltage collapse. The role of high and low field regions within the collector on lowering the terminal voltage has been investigated in reverse biased transistor. An analytical model developed on the basis of the numerical results shows the physics of the phenomenon and the role played by the region of the collector where the generation is absent. Analytical expressions for voltages in different regions within

the collector have clearly revealed that the region where electrons and holes move with their saturated velocities and the carrier generation is negligible, is the main contributor to the negative characteristics and is responsible for causing the experimentally observed low holding voltage. It is also shown that the holding voltage is a function of collector epitaxial layer thickness. This result verifies the experimental observations that the holding voltage increases with the increase of epitaxial layer thickness. The analytical analysis shows that the holding voltage is independent of doping which is also in agreement with experimental observation.

The results of this work would give the designers of power transistor circuits a scope to select necessary protection of the device from CSB. Simple relationships discussed will make their task easier in choosing the device ratings. Also in fabrication process, for increasing the working voltage of transistors the designers may use the relationships as a begining tool for their more complex analysis.

Bibliography

1. C. G. Thornton and C. D. Simmons, " A new high current mode of transistor operation," IRE Trans. Electron. Devices, Vol. ED-5, Jan., pp. 6-10, 1958.

2. Ph. Leturcq and C. Cavalier, " A thermal model for high power devices design," IEDM Tech. Digest, Washington, pp. 422-446, 1974.

3. G. Roman, " A model for computation of second breakdown in transistors," Solid State Electron. 13, pp. 961-980, 1970.

4. D. Stolnitz, " Experimental demonstration and theory of a corrective to second breakdown in Si power transistors," IEEE Trans. Electron. Devices, ED - 13, August/September, pp. 643-648, 1966.

5. H.B. Grutchfield, and T. J. Moutoux, " Current mode second breakdown," IEEE Trans. Electron. Devices, ED - 13, No.11, pp. 743-748, 1966.

6. P. L. Hower and V. G. K. Reddi, " Avalanche injection and second breakdown in transistors," IEEE Trans. Electron. Devices, ED - 17, No.4, pp. 320-335, 1970.

7. D. M. Dow and K. I. Nuttall, " An investigation of the damage produced in epitaxial transistors by second breakdown mechanisms," Int. J. Electronics, Vol. 50, No. 5, pp. 339-351, 1981.

8. D. M. Dow and K. I. Nuttall, " A study of the current distribution established in epitaxial transistors," Int. J. Electronics, Vol. 50, No. 2, pp. 93-108, 1981.

9. I. Dunn and K. I. Nuttall, " An investigation of the voltage sustained by epitaxial bipolar transistor in current mode second breakdown," Int. J. Electronics, Vol. 45, No. 4, pp. 353-372, 1978.

10. J. E. Carroll and P. J. Probert, " Current/voltage characteristics of transistors operating in current mode second breakdown," Solid - State and Electron Devices, Vol. 3, No. 2, pp. 41-48, 1979.

11. B. A. Beatty, S. Krishna, and M. S. Adley," Second breakdown in power transistors due to avalanche injection," IEEE Trans. Electron. Devices, ED - 23, pp. 851-857, 1976.

12. M. M. Shahidul Hassan and H. Domingos, " Estimate of peak

voltage for triggering current mode second breakdown of BJTs during inductive turnoff," Int. J. Electronics, Vol. 66, No. 3, pp. 361-369, 1989.

13. H. A. Schafft, " A survey of second breakdown," IEEE Trans, ED - 13, pp. 613-618, 1966.

14. C. T. Kirk, " A theory of transistors cut-off frequency fall off at UHF transistor at high currents," IRE Trans., ED-9, pp. 164-173, 1969.

15. R. Van Overstreaton and H. de Man, " Measurement of the ionization rates in defused silicon p-n junctions," Solid State Electron., Vol. 13, No. 5, pp. 583-608, 1970.

16. R. Hall, " The effective carrier ionization co-efficient in silicon p-n junctions at breakdown," Int. J. Electronics, Vol. 22, No. 6, pp. 521-528, 1967.

Appendix A

Calculation of electric field E_2

The electric field E_2 at the boundary point x_5 can be determined from the generation integral given by

$$\int_{x_4}^{x_5} g dx = \int_{x_4}^{x_5} (\alpha - \beta) J_n dx + \int_{x_4}^{x_5} \beta J dx \tag{A.1}$$

The right side of the above equation cannot be solved without further assumption. Since the electron multiplication in this region is small, it does not seem unreasonable to assume $J_n = J_{ns}$ for carrying out the integration of the right side of eqn. (A.1)

Following the method outlined in [12] for evaluation of the integral for the small multiplication case, eqn.(A.1) can be integrated by parts, and after neglecting the residual integral, the final form of the integration can be written as

$$\int_{x_4}^{x_5} g dx = E_2^2 \left(\frac{J}{M_n K} \right) \left(\frac{a_n}{b_n} \exp(-\frac{b_n}{E_2}) + \frac{a_h}{b_h} (M_n - 1) \exp(-\frac{b_h}{E_2}) \right) \tag{A.2}$$

where $K = (J - J_o)/2v_s$ is the slope of the electric field in region 5.

Using eqn. (3-67) and eqn. (3-68), it can be shown that

$$E_2^2 \left(\frac{a_n}{b_n} \exp(-\frac{b_n}{E_2}) + \frac{a_h}{b_h} (M_n - 1) \exp(-\frac{b_h}{E_2}) \right) = \left(\frac{M_n}{16 \epsilon v_s J} \right) (J - J_o)^2 \tag{A.3}$$

Appendix B

Calculation of maximum electric field E_m

For multiplication started by electrons, the electron multiplication factor can be written as [15]

$$1 - \frac{1}{M_n} = \int_0^{\bar{x}_m} \alpha \exp\left(-\int_0^x (\alpha - \beta) dx'\right) dx \qquad (B.1)$$

Where, $\bar{x}_m$ is the width of the avalanche region. The ionization coefficients can be written as [15] a = $a_n \exp(-b_n/E)$ and B = $a_h \exp(-b_n/E)$. Here, a_n = 7.03 x 10^5 cm^{-1}, b_n = 1.231 x 10^6 V - cm^{-1}, a_h = 1.582 x 10^6 cm^{-1} and b_h = 2.03 x 10^6 V - cm^{-1}.

One difficulty in evaluating the integral is the substantial difference in the values for holes and electrons. An approach which has been fairly successful[16] has been to assume that the individual ionization coefficients for holes and electrons may be replaced by a single effective ionization coefficient. Following the method outlined in [16] and using the experimental data of Van Overstraeton and De Man [15], the effective ionization coefficient is found to be

$$\alpha' = a_\infty \exp(-\frac{b}{E}) \qquad (B.2)$$

where $a = 1.089 \times 10^6$ cm^{-1} and $b = 1.461 \times 10^6$ $V - cm^{-1}$.

On the assumption of a linear field over the whole multiplication region, the right side of eqn. (B.1) is rewritten as

$$1 - \frac{1}{M_n} = \frac{1}{S}\int_{E_m}^{0} \alpha' \, dE \qquad (B.3)$$

With $S = E_m/\bar{x}_m$, the slope of the field. The right side of eqn. (B.3) can be integrated by parts, and after neglecting the fourth term, one gets

$$1 - \frac{1}{M_n} = \left(\frac{a_\infty}{Sb}\right)\left(1 - \frac{2E_m}{b} + \frac{6E_m^2}{b^2}\right)E_m^2 \exp\left(-\frac{b}{E_m}\right) \qquad (B.4)$$

Eqn.(B.4) can be applied in the evaluation of E_m in this case with the slope given by eqn.(3-67). Taking this average slope and rearranging eqn. (B.4), it can be written as

$$E_m^2 \exp\left(\frac{-b}{E_m}\right) = \left(1 - \frac{1}{M_n}\right)\left(\frac{3b}{4\epsilon v_s a_\infty}\right)(J - J_0)\Big/\left(1 - \frac{2E_m}{b} + \frac{6E_m^2}{b^2}\right) \qquad (B.5)$$